

**Large-scale meta-analysis suggests low regional modularity
in lateral frontal cortex.**

Journal:	<i>Cerebral Cortex</i>
Manuscript ID	Draft
Manuscript Type:	Original Articles
Date Submitted by the Author:	n/a
Complete List of Authors:	de la Vega, Alejandro; University of Texas at Austin, Psychology Yarkoni, Tal; University of Texas at Austin, Psychology Wager, Tor; University of Colorado Boulder, Institute of Cognitive Science; Psychology Banich, Marie; University of Colorado Boulder, Institute of Cognitive Science; Psychology
Keywords:	neuroinformatics, informatics, multivariate, prefrontal

1
2
3
4
5
6
7
8
9
10
11
12
13
14
15
16
17
18
19
20
21
22
23
24
25
26
27
28
29
30
31
32
33
34
35
36
37
38
39
40
41
42
43
44
45
46
47
48
49
50
51
52
53
54
55
56
57
58
59
60

Title: Large-scale meta-analysis suggests low regional modularity in lateral frontal cortex.

Alejandro de la Vega^{*1,2,3}, Tal Yarkoni³, Tor D. Wager^{1,2}, and Marie T. Banich^{1,2}

¹Department of Psychology and Neuroscience, University of Colorado Boulder, 80309 ²Institute of Cognitive Science, University of Colorado Boulder, 80309 ³Department of Psychology, University of Texas at Austin, 78712

Contact Information: Alejandro de la Vega, Department of Psychology, University of Texas at Austin, 108 E. Dean Keeton Stop A8000, Austin, TX 78712, 650-315-9536, email: delavega@utexas.edu

Running title: Large-scale LFC meta-analysis

Abstract

Extensive fMRI study of human lateral frontal cortex (LFC) has yet to yield a consensus mapping between discrete anatomy and psychological states, partly due to the difficulty of inferring mental states from brain activity. Despite this, there have been few large-scale efforts to map the full range of psychological states across the entirety of LFC. Here, we used a data-driven approach to generate a comprehensive functional-anatomical mapping of LFC from 11,406 neuroimaging studies. We identified putatively separable LFC regions on the basis of whole-brain co-activation, revealing 14 clusters organized into three whole-brain networks. Next, we generated preferential psychological profiles by using multivariate classification to identify the psychological states that best predicted activity within each cluster. We observed large functional differences between networks, suggesting brain networks support distinct modes of processing. Within each network, however, we observed relatively low functional specificity, suggesting discrete psychological states are not strongly localized to individual regions; instead, our results are consistent with the view that individual LFC regions work as part of parallel, distributed networks to give rise to flexible behavior. Collectively, our results provide a comprehensive synthesis of a diverse neuroimaging literature using relatively unbiased data-driven methods.

1
2
3
4
5
6
7
8
9
10
11
12
13
14
15
16
17
18
19
20
21
22
23
24
25
26
27
28
29
30
31
32
33
34
35
36
37
38
39
40
41
42
43
44
45
46
47
48
49
50
51
52
53
54
55
56
57
58
59
60

Decades of research have suggested lateral frontal cortex (LFC) plays a critical role in the execution of flexible, goal-directed behavior (Miller and Cohen, 2001), enabling the navigation of complex, rapidly changing environments, pursuit of distant goals in the face of various obstacles, planning for future events, and the communication of complex ideas using language. Although extensive work has identified putatively separable psychological processes critical for flexible behavior (Miyake et al., 2000), the precise organization of these processes within discrete lateral frontal anatomy remains actively debated.

Much progress has been made in understanding the LFC's functional organization by identifying putatively separable subregions on the basis of properties that constrain information processing. For instance, discrete regions have been proposed based on differences in microstructural properties (e.g. cytoarchitecture, (Petrides, 2005), and anatomical (Sallet et al., 2013; Neubert et al., 2015; Orr et al., 2015) and resting-state functional connectivity (Kim et al., 2010; Goulas et al., 2012). Although these studies carefully characterized important functional properties of LFC, it is unclear to what extent the boundaries derived from such methods correspond to the organization of brain activity observed during behavior (Eickhoff et al., 2007).

One approach used to map the functional correlates of distinct behavioral phenotypes is the quantitative meta-analysis of functional MRI (fMRI) studies. Such meta-analyses help overcome the low power observed in individual studies and produce more precise spatial maps of psychological states that activate LFC,

such as working-memory (Wager and Smith, 2003; Nee et al., 2013), inhibition (Nee et al., 2007), switching (Wager et al., 2004; Derrfuss et al., 2005), language (Binder et al., 2009), mentalizing (Gilbert et al., 2006) and self-referential processing (Denny et al., 2012). However, due to the effort required to compile studies, and because most researchers are interested in a particular psychological domain, most meta-analyses are typically focused on a particular LFC subregion or a subset of psychological processes.

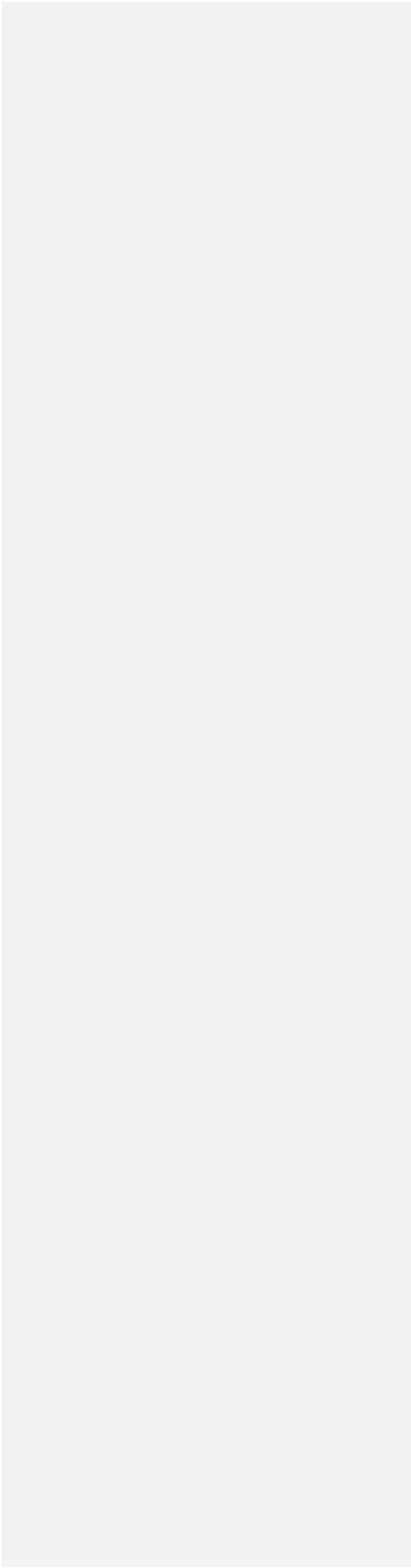
The narrow scope of most existing meta-analyses necessarily limits their impact for two reasons. First, complex behavior likely results from the coordinated activity of individual regions participating across whole-brain networks (Petersen and Sporns, 2015); thus, it is critical to interpret the function of each region in a broader context to better identify subtle differences between similar regions within the same network. Second, it is notoriously difficult to infer mental function from brain activity (the so-called problem of “reverse inference” (Poldrack, 2006), as determining the relative specificity with which a particular task activates a given region requires the ability to quantify the likelihood of activation in that region across a wide range of potential tasks. This problem is particularly acute in brain regions that activate frequently across a broad range of tasks. Hence, the fact that LFC appears to be involved in a broad range of tasks—putatively due to its critical role in guiding flexible behavior (Miller and Cohen, 2001; Dosenbach et al., 2006; Duncan, 2010)—implies that this area may be particularly difficult to associate with specific mental operations (Nelson et al., 2010).

1
2
3
4
5
6
7
8
9
10
11
12
13
14
15
16
17
18
19
20
21
22
23
24
25
26
27
28
29
30
31
32
33
34
35
36
37
38
39
40
41
42
43
44
45
46
47
48
49
50
51
52
53
54
55
56
57
58
59
60

Here we address these issues by creating a comprehensive mapping between data-derived semantic topics representing psychological states and LFC using Neurosynth (Yarkoni et al., 2011), a framework for large-scale fMRI meta-analysis composed of nearly 11,500 studies. First, we used a data-driven method that exploits the observation that functionally related regions co-activate across studies (Toro et al., 2008; Kober and Wager, 2010; Wager et al., 2015; De La Vega et al., 2016; Pauli et al., 2016) to cluster voxels into putatively separable subregions. We applied clustering at two spatial scales, identifying three distinct whole brain networks in LFC composed of several smaller subregions with dissociable co-activation patterns. We then characterized the functional profile of each resulting region using multivariate classification, contrasting studies that activated each region with those that did not, resulting in psychological profiles for each LFC subregion. Collectively, we provide a comprehensive and relatively unbiased meta-analytic functional-anatomical mapping of LFC.

Materials and Methods

Dataset. We analyzed version 0.6 of the Neurosynth database (Yarkoni et al., 2011), a repository of 11,406 fMRI studies and over 410,000 activation peaks that span the full range of the published neuroimaging literature. Each observation contains the peak activations for all contrasts reported in a study’s table as well as the frequency of all of the words in the article abstract. A heuristic but relatively accurate approach is used to detect and convert reported coordinates to the standard MNI space. As such, all activations and subsequent analyses are in MNI152 coordinate space. The scikit-learn Python package (Pedregosa et al., 2011)



was used for all machine learning analyses. Analyses were performed using the core Neurosynth python tools (<https://github.com/neurosynth/neurosynth>). Code and data to replicate these analyses on any given brain region at any desired spatial granularity are available as a set of IPython Notebooks (<https://github.com/adelavega/neurosynth-lfc>).

Lateral frontal cortex mask. To select clusters from whole-brain clustering solutions in lateral frontal cortex, we defined an LFC anatomical mask. Crucially, we only used this mask to select clusters that fell within this mask, and not to exclude individual voxels. First, we included voxels with a greater than 30% chance of falling in the frontal lobes according to the Montreal Neurological Institute structural probabilistic atlas and excluded medial voxels within 14mm of the midline. To focus on lateral frontal cortex, we excluded voxels that were exclusively located on the orbital surface—ensuring to include lateral orbitofrontal voxels—by removing voxels in the superior and medial orbital gyri according to the AAL atlas and voxels with a greater than 30% probability of falling in ‘Frontal Operculum Cortex’ in the Harvard-Oxford atlas. Finally, we also excluded far ventral voxels of OFC ($Z < -14\text{mm}$) that were not excluded using anatomical atlases.

Co-activation clustering. Next, we clustered individual grey-matter cortical voxels across the whole brain based on their meta-analytic co-activation with the whole brain across studies in the database (Figure 1a). In order to avoid potentially biased or arbitrary cluster boundaries, we clustered the whole cortex and selected clusters for further analysis that fell within an anatomically defined LFC mask.

1
2
3
4
5
6
7
8
9
10
11
12
13
14
15
16
17
18
19
20
21
22
23
24
25
26
27
28
29
30
31
32
33
34
35
36
37
38
39
40
41
42
43
44
45
46
47
48
49
50
51
52
53
54
55
56
57
58
59
60

Critically, we did not mask out voxels that were slightly outside of our mask– we either included or excluded entire clusters. This was particularly important for clusters near the edge of our LFC mask– as functional boundaries may not conform to anatomical boundaries– and at coarse clustering solutions– given the well-established finding that at least 4-5 whole-brain networks include voxels in lateral frontal cortex (Yeo et al., 2011). For whole-cortex clustering, we excluded voxels with less than 30% probability of falling in grey matter according to the Harvard-Oxford anatomical atlas and those with very low activation in the database (less than 100 studies per voxel). In general, Neurosynth’s activation mask (derived from the standard MNI152 template distributed with FSL) highly corresponded with probabilistic locations of cerebral cortex, with the exception of portions of dorsal precentral gyrus– which showed relatively infrequent activation.

We calculated the co-activation between each cortical voxel and every other voxel in the brain (including sub-cortex) by determining how correlated their activity was across studies. Activation in each voxel is represented as a binary vector of length 11,406 (the number of studies). A value of 1 indicated that the voxel fell within 10 mm of an activation focus reported in a particular study, and a value of 0 indicated that it did not. Because correlating the activation of every cortical voxel with every other voxel in the brain would result in a very large matrix (112,358 cortical voxels x 171,534 whole-brain voxels) that would be very computationally costly to cluster so as to identify distinct LFC regions. Hence, we reduced the dimensionality of the whole brain to 100 components using principal components analysis (PCA; the

precise choice of number of components does not materially affect the reported results). Next, we computed the Pearson correlation distance (the inverse of Pearson correlation) between every voxel in the LFC mask with each whole-brain PCA component, resulting in a matrix that described the frequency with which each cortical voxel co-activated with the rest of the brain.

As an additional pre-processing step, we standardized each cortical voxel's co-activation with other brain voxels to ensure clustering would be driven by relative differences in whole brain co-activation and not the overall activation rate of each voxel. That is, if two voxels co-activated with similar voxels across the brain, we should consider them to be relatively similar even if one of those voxels activates more frequently (and thus has slightly stronger correlations with all voxels). This adjustment was particularly important, as preliminary analyses indicated that regions with very high rates of activation (e.g. pre-SMA/mid-cingulate cortex) more readily clustered into multiple clusters with few voxels, reflecting base rates in activation, although differences in their functional associations were minimal. Indeed, preliminary analyses confirmed that standardizing the co-activation matrix alleviated this concern. At $k = 70$, the mean activation rate of each cluster showed no correlation with voxel size when Z-scoring was used ($r=0.05$), as compared to when the raw co-activation matrix was used ($r = -0.65$) at $k = 70$. Additionally, the range of cluster sizes was compressed, resulting in more evenly sized clusters. Cluster sizes ranged from 352 to 4546 voxels using the raw activation, compared to a range of 560 to 2862 voxels using standardized co-activation.

1
2
3
4
5
6
7
8
9
10
11
12
13
14
15
16
17
18
19
20
21
22
23
24
25
26
27
28
29
30
31
32
33
34
35
36
37
38
39
40
41
42
43
44
45
46
47
48
49
50
51
52
53
54
55
56
57
58
59
60

We applied hierarchical clustering with Ward’s linkage to the normalized co-activation matrix, resulting in a whole-brain linkage matrix. Ward’s clustering was selected as this algorithm is recommended as a good compromise between accuracy (e.g., fit to data) and reproducibility for clustering fMRI data (Thirion et al., 2014). However, this clustering algorithm is seldom used for whole-brain clustering because the computational time increases cubically [$\Theta(N^3)$] as a function of samples. We employed the fastcluster algorithm (Müllner, 2013)—a package of libraries that enable efficient hierarchical clustering [$\Theta(N^2)$ —to achieve whole-brain clustering.

Since the optimality of a given clustering depends in large part on investigators’ goals, the preferred level of analysis, and the nature and dimensionality of the available data, identifying the ‘correct’ number of clusters is arguably an intractable problem (Eickhoff et al., 2015). However, in order to attempt to objectively guide the choice of number, we selected viable solutions using the silhouette score— a measure of within-cluster cohesion. Crucially, as we were specifically interested in the fit of the clustering to lateral frontal cortex, we only calculated the silhouette score with respect to voxels within our lateral frontal cortex mask. The silhouette coefficient was defined as $(b - a) / \max(a, b)$, where a is the mean intra-cluster Euclidian distance and b is the distance between a sample and the nearest cluster of which the sample is not a part. Solutions that minimized the average Euclidian distance between voxels within each cluster received a greater score. Once having chosen two spatial scales, we extracted flat LFC clusters from with a substantial percentage of

Comment [AD1]: Define distance

voxels within our apriori LFC mask. We varied the percentage of voxels within our LFC mask required to include a region across granularities with the objective maximizing coverage in LFC without including extraneous clusters with little presence in LFC. We arrived at 12% of voxels in a cluster within LFC at $k=5$ and 75% of voxels at $k=70$.

To understand the anatomical correspondence of the resulting clusters, we consulted a variety of anatomical and cytoarchitectonic atlases. To locate each cluster anatomically, we used the probabilistic Harvard-Oxford atlas (H-O) that is packaged with FSL. We also visually compared the location of our clusters to the Petrides' (2005) and Jülich micro-anatomical atlases included in FSL (Eickhoff et al., 2007). Regions were assigned names in accordance to Brodmann areas (BA) whenever clusters were sufficiently small to correspond to a single area (e.g. 'area 9/46v'). Clusters were given functional names when they spanned multiple cytoarchitectonic areas (e.g. IFJ) or multiple clusters spanned a single cytoarchitectonic area (e.g. PMd & PMv). Note that although names were assigned to ease the discussion of these regions, we do not make strong claims of correspondence between functionally and anatomically defined regions, as we observed several discrepancies throughout LFC.

Co-activation profiles. Next, we analyzed the differences in whole brain co-activation between the resulting clusters (Figure 1b) in order to understand the patterns of co-activation that differentiates these clusters. To highlight differences

1
2
3
4
5
6
7
8
9
10
11
12
13
14
15
16
17
18
19
20
21
22
23
24
25
26
27
28
29
30
31
32
33
34
35
36
37
38
39
40
41
42
43
44
45
46
47
48
49
50
51
52
53
54
55
56
57
58
59
60

between clusters, we contrasted the co-activation of each cluster to the mean co-activation of the entire LFC. To do so, we performed a meta-analytic contrast between studies that activated a given cluster, and studies that activated a LFC mask composed of all clusters. The resulting images identify voxels with a greater probability of co-activating with the cluster of interest than with LFC on average. For example, voxels in blue in Figure 5b indicate voxels that are active more frequently in studies in which ‘area 9’ is active than in studies in which other LFC on average is active. We calculated p-values for each voxel using a two-way chi-square test between the two sets of studies and thresholded the co-activation images using the False Discovery Rate ($q < 0.01$). The resulting images were binarized for display purposes and visualized using the pysurfer Python library.

Topic modeling. Although term-based meta-analysis maps in Neurosynth closely resemble the results of manual meta-analyses of the same concepts, there is a high degree of redundancy between terms (e.g. ‘episodes’ and ‘episodic’), as well as potential ambiguity as to the meaning of an individual word out of context (e.g. ‘memory’ can indicate working memory or episodic memory). To remedy this problem, we employed a reduced semantic representation of the latent conceptual structure underlying the neuroimaging literature: a set of 60 topics derived using latent dirichlet allocation (LDA) topic-modeling (Blei et al., 2003). This procedure was identical to that used in a previous study (Poldrack et al., 2012), except for the use of a smaller number of topics and a much larger version of the Neurosynth database. The generative topic model derives 60 independent topics from the co-

occurrence of all words in the abstracts of fMRI studies in the database. Each topic loads onto individual words to a varying extent, facilitating the interpretation of topics; for example, a working memory topic loads highest on the words “memory, WM, load”, while an episodic memory topic loads on “memory, retrieval, events”. Note that both topics highly load on the word “memory”, but the meaning of this word is disambiguated because it is contextualized by other words that strongly load onto that topic. Although the set of topics included 25 topics representing non-psychological phenomena—such as the nature of the subject population (e.g. gender, special populations) and methods (e.g., words such as “images”, “voxels”)—these topics were not explicitly excluded as they were rarely the strongest loading topics for any region. For all of our results, we focus on a set of 16 topics that strongly loaded onto lateral frontal cortex clusters (Table 1). These topics were obtained by determining the two strongest loading topics for each region.

Meta-analytic functional preference profiles. We generated functional preference profiles by determining which psychological topics best predicted each cluster’s activity across fMRI studies (Figure 1c). First, we selected two sets of studies: studies that activated a given cluster—defined as activating at least 5% of voxels in the cluster— and studies that did not— defined as activating no voxels in the cluster. For each cluster, we trained a naive Bayes classifier to discriminate these two sets of studies based the loading of psychological topics onto individual studies. We chose naive Bayes because (i) we have previously had success applying this algorithm to Neurosynth data (Yarkoni et al., 2011); (ii) these algorithms

1
2
3
4
5
6
7
8
9
10
11
12
13
14
15
16
17
18
19
20
21
22
23
24
25
26
27
28
29
30
31
32
33
34
35
36
37
38
39
40
41
42
43
44
45
46
47
48
49
50
51
52
53
54
55
56
57
58
59
60

perform well on many types of data, (iii) they require almost no tuning of parameters to achieve a high level of performance; and (iv) they produce highly interpretable solutions, in contrast to many other machine learning approaches (e.g., support vector machines or decision tree forests).

We trained models to predict whether or not fMRI studies activated each cluster, given the semantic content of the studies. In other words, if we know which psychological topics are mentioned in a study how well can we predict whether the study activates a specific region? We used 4-fold cross-validation for testing and calculated the mean score across all folds as the final measure of performance. We scored our models using the area under the curve of the receiver operating characteristic (AUC-ROC)– a summary metric of classification performance that takes into account both sensitivity and specificity. AUC-ROC was chosen because this measure is not detrimentally affected by unbalanced data (Jeni et al., 2013), which was important because each region varied in the ratio of studies that activated it to the studies that did not.

To generate functional preference profiles, we extracted from the naive Bayes models the log odds-ratio (LOR) of a topic being present in active studies versus inactive studies. The LOR was defined, for each region, as the log of the ratio between the probability of a given topic in active studies and the probability of the topic in inactive studies, for each region. LOR values above 0 indicate that a psychological topic is predictive of activation of a given region. To determine the statistical significance of these associations, we permuted the class labels and

extracted the LOR for each topic 1000 times. This resulted in a null distribution of LOR for each topic and each cluster. Using this null distribution, we calculated p-values for each pairwise relationship between psychological concepts and regions, and reported associations significant after controlling for multiple comparisons using False Discovery Rate with $q < 0.01$. Finally, to determine if certain topics showed greater preference for one cluster versus another, we conducted exploratory, post-hoc comparisons by determining if the 95% confidence intervals (CI) of the LOR of a specific topic for a one region overlapped with the 95% CI of the same topic in another region. We generated CIs using bootstrapping, sampling with replacement and recalculating log-odds ratios for each region 1000 times. A full reference figure of the loadings between topic and regions, including CIs, is available in Supplemental Figure 3. A full reference of the CIs of each associations is available in the online repository, along with code to generate such CIs for any given region.

Results

Hierarchical clustering of lateral frontal cortex. We identified spatially dissociable regions on the basis of shared co-activation profiles with the rest of the brain (Toro et al., 2008; Kober and Wager, 2010; Wager et al., 2015; De La Vega et al., 2016; Pauli et al., 2016), an approach that exploits the likelihood of a voxel co-activating with other voxels across studies in the meta-analytic database. To identify whole-brain networks spanning beyond LFC, we applied hierarchical

1
2
3
4
5
6
7
8
9
10
11
12
13
14
15
16
17
18
19
20
21
22
23
24
25
26
27
28
29
30
31
32
33
34
35
36
37
38
39
40
41
42
43
44
45
46
47
48
49
50
51
52
53
54
55
56
57
58
59
60

clustering to the whole cortex and selected clusters within LFC mask for further analysis (Figure 2b). In order to map structure to function across various spatial scales, we extracted 4– to 100– whole-brain clusters and evaluated their quality using the silhouette score, a measure of intra-cluster cohesion (Kober et al., 2008; Pauli et al., 2016) (Figure 2a). Given the intractable nature of choosing the ‘correct’ number of clusters (Eickhoff et al., 2015) and the lack of a single dominant solution in our data, we focused on two well spaced granularities, 5 and 70 whole-brain clusters, avoiding low quality solutions (i.e. 7-38 clusters). Importantly, we do not argue that the solutions we selected are in any way privileged, nor did we aim to match the scale of previous parcellations; rather, we simply chose two spatial scales for subsequent analysis with distinct vantage points into the hierarchical organization of LFC.

To understand the large-scale network organization of LFC, we focus on the five-cluster solution as this scale exhibited the greatest silhouette score of coarse network-level solutions. Three of these whole-brain network clusters were present in LFC (Figure 2c) and showed moderate correspondence to previously described large-scale networks (Yeo et al., 2011)

The largest of the three clusters, which we refer to as the “fronto-parietal” network, spanned half of LFC, primarily in prefrontal cortex, and resembled Yeo et al., 2011’s description of the “fronto-parietal” network (Yeo et al., 2011) (dice coefficient (d) = 0.56). Additionally, this cluster spanned medial-frontal and anterior

insular aspects of the “ventral attention” network ($d = 0.21$). A second cluster, which we refer to as the “default” network, closely matched extensive descriptions of the “default” or “task negative” network ($d = 0.62$) (Andrews-Hanna, 2012). The final cluster, which we refer to as the “sensorimotor” network, was located in posterior LFC and showed moderate overlap with Yeo’s “somatosensory-motor” network ($d = 0.36$) and, to a lesser extent, the “dorsal attention network” ($d=0.31$).

Having identified large-scale networks in LFC, we sought to identify more functionally specific subregions within each network with potentially dissociable psychological profiles. Although the silhouette values indicated that inter-cluster cohesion continuously increases with number of clusters, we chose to focus on a spatial scale that balanced clustering quality with psychological interpretability. Thus, we chose to focus on the 70- cluster solution, as this was the coarsest scale to result in a set of largely spatially contiguous LFC clusters. From these 70 whole brain clusters, we identified 14 clusters within our LFC mask (Figure 2d), hierarchically organized into the coarser large-scale networks (see Supplemental Figure 1 for whole-brain cluster results).

To provide direct insight into the functions of the 14 LFC fine-grained clusters we identified, we applied two approaches. First, we determined which voxels across the brain differentially co-activated with each cluster, revealing distinct patterns of whole brain co-activation. Second, we used semantic data from Neurosynth to determine which latent psychological topics predict the activation of each cluster,

1
2
3
4
5
6
7
8
9
10
11
12
13
14
15
16
17
18
19
20
21
22
23
24
25
26
27
28
29
30
31
32
33
34
35
36
37
38
39
40
41
42
43
44
45
46
47
48
49
50
51
52
53
54
55
56
57
58
59
60

resulting in a meta-analytic psychological preference profile for each subregion.
Next, we step through these results separately for each network.

Fronto-parietal network

The majority of lateral frontal cortex belonged to the frontal extent of the “fronto-parietal” network, which further spanned portions of lateral parietal cortex, anterior insula, pre-SMA, mid-cingulate cortex (MCC), and the precuneus. Within LFC, we identified 10 finer-grained subregions within the “fronto-parietal” network. For purely illustrative purposes, we used the hierarchical clustering dendrogram (Figure 2b) to identify a granularity in which these clusters formed three sets; at $k = 24$ whole brain clusters, these 10 LFC clusters organized into three groups: caudal, mid and rostral regions. Across these three groupings, all clusters showed robust associations with executive functions, although we observed subtle variations in psychological preferences.

In caudal LPFC, we identified two adjacent bilateral clusters (Figure 3a). The most posterior of the two (‘6/8’) was located anterior to the premotor cortex and extended from lateral superior frontal gyrus to the intermediate frontal sulcus of middle frontal gyrus. This cluster overlapped with functional descriptions of the frontal eye fields (FEF)– a region important for volitional eye saccades (Paus, 1996). Immediately anterior, we identified a cluster (‘9/46c’) spanning caudal area 9/46 from the intermediate frontal sulcus into caudal portions of 9/46v. Notably, although cluster ‘9/46c’ arguably extends well into “mid” LPFC, this cluster did not

group with other mid-LPFC clusters until much coarser granularities, suggesting these clusters may exhibit distinct functional signatures despite their spatial proximity.

Anterior and ventral to caudal LPFC, we identified four clusters spanning common definitions of ‘mid’ lateral prefrontal cortex (Figure 3b). The organization of clusters in this region, however, varied by hemisphere. Most dorsally, we identified a mostly left-lateralized cluster (‘9/46v’), extending from the intermediate frontal sulcus into the fundus of the inferior frontal sulcus. Next, we identified a cluster, which we refer to as right IFG (‘IFG [R]’), spanning the majority of area BA45 in the right hemisphere. Notably, only right IFG was part of the fronto-parietal network, consistent with the observation that this region is consistently observed during goal-directed cognition. Posterior to these two clusters, we identified a bilateral cluster consistent with the inferior frontal junction (‘IFJ’) (e.g. MNI coordinates: 48, 4, 33 (Muhle-Karbe et al., 2016), located in the fundus of caudal inferior frontal sulcus, extending into precentral, inferior frontal and middle frontal gyri. Finally, ventral to this cluster, but only in the right hemisphere, we identified a fourth cluster (‘44 [R]’) located in posterior IFG, spanning BA44 and abutting BA6.

In ‘rostral’ LPFC, we identified three bilateral clusters spanning BA10 (Figure 3c). These three clusters were organized along a ventral-dorsal axis, consistent with a prior DTI parcellation (Orr et al., 2015), and were exclusively in lateral frontal cortex, consistent with cytoarchitectonic evidence of a lateral-medial

1
2
3
4
5
6
7
8
9
10
11
12
13
14
15
16
17
18
19
20
21
22
23
24
25
26
27
28
29
30
31
32
33
34
35
36
37
38
39
40
41
42
43
44
45
46
47
48
49
50
51
52
53
54
55
56
57
58
59
60

distinction of the frontal pole (Bludau et al., 2014). The most dorsal cluster ('9/46dr') extended into rostral portions of BA 9/46, while the next two clusters ('10v' and '10d') were exclusively located in BA 10, separated along a dorsal/ventral axis

Meta-analytic co-activation. To better understand functional differences between these regions, we directly contrasted the co-activation of each cluster with that of LFC as whole in order to identify voxels across the brain that differentially co-activated with each cluster (Figure 3; right panel). We observed that most differential co-activation occurred within other cortical association cortex areas such as lateral parietal cortex (LPC), pre-SMA and MCC, and the insula. Across LPC, each LFC cluster co-activated most strongly with distinct areas across a gradient extending from tempo-parietal junction to the lateral parieto-occipital sulcus. For example, clusters '9/46c' and all fronto-polar clusters showed greater co-activation with parietal cortex ventral to the intraparietal sulcus. In contrast, area '6/8' and all four 'mid' LPFC clusters showed greater co-activation within and dorsal to the intraparietal sulcus.

Similarly in medial PFC, all clusters except right IFG and '9/46dr' co-activated most strongly with slightly different portions of pre-SMA and MCC. Generally, more anterior clusters co-activated more strongly with more anterior portions of pre-SMA/MCC. For instance, '10d' co-activated most strongly with a anterior mid-cingulate cortex while '44 [R]' co-activated most strongly with the SMA. Finally, in the insula, several LFC subregions exhibited differential co-

activation with distinct sub-divisions of the insula. For example, cluster '44 [R]' co-activated most strongly with the posterior insula– an important region for pain and sensorimotor processing (Chang et al., 2013)– whereas IFJ co-activated most strongly with the dorsal anterior insula, a subregion implicated in goal-directed cognition. In contrast, area 10v showed greater co-activation with ventral anterior insula, an area implicated in affect (Chang et al., 2013).

This observation that the bulk of co-activation differences between LFC subregions of the fronto-parietal network occurred within other cortical association areas is consistent with the hypothesis that association cortex is composed of parallel interdigitated networks (Yeo et al., 2011). That is, these findings suggest subregions of the FPN do not participate with categorically distinct sets of regions across the brain, and instead perform subtly different roles within a distributed network.

Meta-analytic functional preference. Next, we used a data-driven approach that surveyed a broad range of fMRI studies to quantify the degree to which distinct psychological states might be preferentially associated with different LFC clusters (Figure 1c). We trained naïve Bayes classifiers to predict the presence or absence of activation in each LFC cluster using a set of 60 psychological topics derived by applying a standard topic modeling approach to the abstracts of articles in the Neurosynth database (Poldrack et al., 2012). We used the fitted model coefficients to quantify the strength of association between each psychological topic

1
2
3
4
5
6
7
8
9
10
11
12
13
14
15
16
17
18
19
20
21
22
23
24
25
26
27
28
29
30
31
32
33
34
35
36
37
38
39
40
41
42
43
44
45
46
47
48
49
50
51
52
53
54
55
56
57
58
59
60

and the presence of activation in the corresponding LFC cluster (measured as the log odds-ratio [LOR] of the probability of each topic in studies that activated a given cluster relative to the probability of the same topic in studies that did not activate the cluster). Values greater than 0 indicate that the presence of that topic in a study positively predicts activity in a given region. We report the results of 16 psychological topics that loaded strongly onto LFC regions (Table 1) and restrict interpretation to significant associations using False Discovery Rate (FDR; $q < 0.01$). In addition, whenever we comparatively discuss sets of regions, we discussed differences if the 95% confidence interval (CI) of a given topic did not overlap between two regions (Supplemental Figure 3). As the latter comparisons are post-hoc and exploratory, caution in interpretation is warranted.

Consistent with a distributed role for the fronto-parietal network in goal-directed cognition, all nine clusters were significantly associated with working-memory, all clusters except 10d and 10v were associated with conflict, and seven clusters were associated with switching (Figure 4). The present results are inconsistent with focal anatomical locations for high-level executive processes; instead, these results suggest that distributed activation across fronto-parietal network supports goal-directed cognition in the face of interference and conflict (Nee and Brown, 2012). Despite the relatively low modularity we observed across the fronto-parietal network, multivariate associations between individual subregions and psychological states suggest preferential functional correlates can be identified for each cluster.

Caudal fronto-parietal LFC. Consistent with its co-location with the frontal eye fields, '6/8' was the only cluster significantly associated with saccadic eye movements (i.e. 'gaze') in the fronto-parietal network, and was also associated with 'attention'. This pattern suggests that area '6/8' may be important for directing attention to relevant external stimuli to support downstream information processing. However, '6/8' was also significantly associated with a 'working-memory' topic, consistent with a recent lesion study implicating the FEF in a causal role in working memory (Mackey et al., 2016). These results suggest area '6/8' is not merely involved in low-level saccadic eye movements, but plays an important role in higher-level cognition.

In contrast, cluster '9/46c' showed a much less distinctive functional signature, with relatively weak associations to other psychological processes outside of core EF processes and 'memory'. This relatively diffuse pattern suggests area '9/46c' may be involved in domain-general processes that span across distinct psychological states in our topic model.

Mid fronto-parietal LFC. Clusters '9/46v' and IFJ showed similar functional profiles, exhibiting robust associations with several executive functions (e.g. 'working memory', 'conflict', 'switching') in addition to 'semantics'. Cluster '9/46v' showed a particularly strong association with executive functions— exhibiting the strongest relationship across LFC with 'conflict'; these results are consistent with a hypothesized role for mid-DLPFC as a seat of high-level executive processes (Petrides, 2005).

1
2
3
4
5
6
7
8
9
10
11
12
13
14
15
16
17
18
19
20
21
22
23
24
25
26
27
28
29
30
31
32
33
34
35
36
37
38
39
40
41
42
43
44
45
46
47
48
49
50
51
52
53
54
55
56
57
58
59
60

These results are also consistent with the hypothesis that IFJ is involved in task-set switching; (Derrfuss et al., 2005) however, given that several other LFC clusters were similarly associated with switching, it is unlikely IFJ is focally responsible for this phenomenon. Yet, IFJ showed a stronger association with low and high level motor function (i.e. ‘motor’, ‘action’) than other fronto-parietal LFC clusters, suggesting that IFJ is important for motoric aspects of cognitive control (De Baene et al., 2012). In contrast, cluster ‘44 [R]’ exhibited weaker associations with executive functions and robust associations with motor function and ‘pain’, suggesting area this area is more involved in sensori-motor processing than high-level cognitive control.

Finally, ‘IFG [R]’ showed a distinct functional signature to other mid LPFC clusters, with much weaker associations with conflict, working memory and switching; instead, ‘IFG [R]’ was associated with ‘inhibition’– consistent with extensive studies linking this region to inhibitory processes (Nee et al., 2013). ‘IFG [R]’ was also associated with ‘emotion’, consistent with the hypothesis that this region is crucial for effective emotion regulation and reappraisal (Wager et al., 2008; Woo et al., 2014). However, the relationship between ‘inhibition’ and ‘IFG [R]’ was not particularly strong or significantly greater than other fronto-parietal regions, suggesting ‘IFG [R]’ may play a more domain general role such as context monitoring (Chatham et al., 2012). Alternatively, local neuronal groups not detectable by fMRI may play more specific and distinct roles (Tye and Deisseroth, 2012; Kvitsiani et al., 2013; Xiu et al., 2014).

Rostral fronto-parietal LFC. Although ‘rostral’ fronto-parietal clusters exhibited significant associations with various executive processes, these three clusters were characterized by weaker associations with motor function (‘action’), language and ‘conflict’. Rather, clusters ‘9/46dr’ and ‘10d’ were robustly associated with ‘inhibition’ and cluster ‘10d’ with ‘novelty’. This pattern of results suggests fronto-polar LFC regions may be important for high-level monitoring and guiding of cognitive control, removed from low-level motor implementations.

Finally, the most ventral fronto-polar region, cluster ‘10v’, showed a more distinct pattern, exhibiting weaker associations with all executive processes but a significant association with ‘reward’ (at a lower threshold, $q < 0.05$). This pattern is consistent with its location near orbitofrontal cluster, and provides support for hypotheses that suggest that the ventral frontal pole may be important for representing the value of appetitive stimuli in order to effectively guide goal-directed behavior (Orr et al., 2015).

Default network

Anatomical correspondence. We identified three distinct default network clusters in LFC, consistent with previous descriptions of the default network and large-scale rs-fMRI parcellations (Figure 5a) (Yeo et al., 2011). The first two clusters were positioned adjacent to each other in ventrolateral prefrontal cortex. The more anterior of the two (‘47/12’) spanned lateral orbitofrontal cortex and IFG orbitalis bilaterally, while a more posterior and dorsal cluster spanned inferior frontal gyrus

1
2
3
4
5
6
7
8
9
10
11
12
13
14
15
16
17
18
19
20
21
22
23
24
25
26
27
28
29
30
31
32
33
34
35
36
37
38
39
40
41
42
43
44
45
46
47
48
49
50
51
52
53
54
55
56
57
58
59
60

exclusively in the left hemisphere ('IFG [L]'). Finally, we identified a third cluster in dorsal LPFC consistent with BA9 (Petrides, 2005), extending from superior frontal gyrus to dorsal middle frontal gyrus across the superior frontal sulcus. This cluster has long been noted for its lack of anatomical input from lateral and medial parietal cortex (Petrides and Pandya, 1984; Cavada and Goldman-Rakic, 1989). Thus, despite these cluster's close proximity to fronto-parietal clusters, we expected them to exhibit very distinct functional profiles.

Meta-analytic co-activation. Consistent with the grouping of these clusters with the default network, clusters '47/12' and '9' co-activated much more strongly than the rest of LFC with other default network regions, such as dorsal medial PFC (mPFC), middle temporal gyrus and angular gyrus (Figure 5b). Area '9' showed particularly robust co-activation with key hubs of the default network, such as anterior mPFC and posterior cingulate cortex (PCC), firmly placing this region in the default network despite its proximity to mid-DLPFC. In contrast, 'IFG [L]' showed a relatively distinct pattern, showing co-activation with portions of the fronto-parietal network— such as mid-DLPFC and pre-SMA. This pattern is consistent with the fact that left IFG's contralateral homologue clustered with the fronto-parietal network and suggests this region may not be entirely dissociable from fronto-parietal clusters. Moreover, left IFG also showed stronger co-activation with posterior superior temporal sulcus— a key region implicated in semantic processing (Binder et al., 2009) suggesting left IFG may also show a preference towards language topics.

Meta-analytic functional preference. In contrast to clusters in the frontal-parietal network, clusters '47/12' and '9' showed no association with any executive processes— particularly notable for cluster '9' due to its spatial proximity to mid fronto-parietal clusters (Figure 5c). Instead, clusters '47/12' and '9' were significantly associated with 'mentalizing', consistent with the hypothesis that these regions, as part of the dorsal medial subsystem of the default network, play an important role in conceptual processing and mentalizing (Andrews-Hanna et al., 2014).

Distinct from other default network clusters, '45 [L]' showed a significant association with various executive functions— further highlighting the distributed nature of executive processes across frontal regions. However, area '45 [L]' was not associated with inhibition, suggesting inhibition is right-lateralized to some degree (Aron et al., 2014). Furthermore, consistent with this region's co-location with Broca's area and co-activation with the superior temporal sulcus, area '45 [L]' was significantly associated with 'semantics' and 'speech'. Importantly, although it well-known Broca's area is important for motor function in language, we did not find any association between area '45 [L]' and motor topics; these results suggest Broca's area is involved in the generation of speech motor plans, but not motor function more generally (Flinker et al., 2015). Moreover, '45 [L]' was notable for its robust association with 'semantic' function— more so than any other region— consistent with the hypothesis that left IFG is a part of the brain's 'semantic' system (Binder et al., 2009).

1
2
3
4
5
6
7
8
9
10
11
12
13
14
15
16
17
18
19
20
21
22
23
24
25
26
27
28
29
30
31
32
33
34
35
36
37
38
39
40
41
42
43
44
45
46
47
48
49
50
51
52
53
54
55
56
57
58
59
60

Finally, consistent with the default network’s well-characterized involvement in memory (Andrews-Hanna et al., 2014), all three LFC default clusters were robustly associated with ‘memory’ and ‘emotion’. This is consistent with a long line of evidence supporting the role of these regions in autobiographical, internally oriented cognition. Moreover, the left IFG is purported to play a key role in controlled memory retrieval (Badre and Wagner, 2007; Snyder et al., 2011)– a hypothesis supported by the joint association between executive processes and memory in this region. However, it is also notable that ‘memory’ was associated with many other clusters in the fronto-parietal network, suggesting memory processes are widely distributed across lateral frontal cortex.

Somatosensory-motor network

We identified two LFC clusters in the somatosensory-motor network: dorsal and ventral lateral premotor cortex– ‘PMd’ and ‘PMv’, respectively (Figure 6a). Both clusters were located in dorsal BA 6 (Eickhoff et al., 2007), although ‘PMd’ was slightly more anterior. As a result of its more posterior location, ‘PMv’ included several voxels in primary motor cortex, although the cluster was primarily located in pre-motor cortex.

Meta-analytic co-activation. Both PMd and PMv showed greater co-activation with nearby voxels in the primary motor and somatosensory cortices, as well as SMA– regions important for the control of movement (Figure 6b). PMd, however, additionally showed greater co-activation with various regions implicated

in executive function, such as lateral parietal cortex and the anterior insula—suggesting dorsal pre-motor cortex may engage a broader functional network in support of the cognitive control of motor actions.

Meta-analytic functional preference. The functional preference profiles of both premotor clusters suggest their primary functional role is in core aspects of motor function (Figure 6c). However, both of these the two clusters were also associated with higher-level motor planning (i.e. ‘action’) and working-memory, suggesting these regions are important for higher-level motoric control. Moreover, consistent with PMd’s stronger co-activation with regions previously associated with executive function, PMd was significantly associated with ‘conflict’ and ‘attention’ (although not significantly more so than PMv). Thus, although these two premotor clusters were most strongly associated with motor function, their function is not exclusively limited to low-level processes, and may require the recruitment of higher-level psychological processes for the execution of motor plans.

Functional distance between clusters

Finally, to examine the overall difference between regions, we computed the mean correlation distance between clusters on the basis meta-analytic co-activation (Figure 7a) and psychological preference profiles (Figure 7b). Supporting the network organization of these clusters, the distance between clusters in the same network was much shorter (co-activation: $r=0.58$, functional profiles, $r=0.5$) than the distance between clusters in different networks (co-activation: $r=0.7$, functional profiles, $r=0.7$) across both modalities. However, the distance between clusters in

1
2
3
4
5
6
7
8
9
10
11
12
13
14
15
16
17
18
19
20
21
22
23
24
25
26
27
28
29
30
31
32
33
34
35
36
37
38
39
40
41
42
43
44
45
46
47
48
49
50
51
52
53
54
55
56
57
58
59
60

the same network was in certain cases relatively high. For example, clusters ‘45 [L]’ and ‘9’ in the default network ($r = 0.77$) and ‘44 [R]’ and ‘10v’ in the fronto-parietal network ($r = 0.93$) exhibited large functional distances, despite belonging to the same network. Thus, although large-scale networks likely represent a fundamental organizational structure in the brain– and distinct networks tend to support categorically different types psychological processes– our results suggest these networks are relatively heterogeneous. Finally, we also observed that the differences between regions based on meta-analytic co-activation were highly similar to those based on functional preference profiles (Pearson’s correlation $r = 0.86$), suggesting that clusters that show distinct meta-analytic co-activation generally exhibit distinct functional preference profiles.

Discussion

In the present study, we applied data-driven methods to the largest meta-analytic database available to systematically map psychological states to discrete lateral frontal cortex anatomy. Importantly, we conducted our analyses broadly both with respect to anatomy– by focusing on the entirety of LFC– and function– by surveying a wide, representative range of psychological states– resulting in a relatively unbiased and comprehensive functional-anatomical mapping. Using co-activation-based hierarchical clustering, we identified 14 subregions in LFC organized into three whole-brain networks (fronto-parietal, default and sensorimotor). We then used multivariate classification to determine which psychological states best predicted activation in each region, resulting in dissociable psychological profiles for each subregion. In contrast with more modular models of

LFC organization (Fodor, 1983; Baddeley, 2003; Bertolero et al., 2015), we observed a complex many-to-many mapping between individual regions and discrete psychological states, suggesting cognitive processes are supported in a distributed fashion by regions organized into whole-brain networks.

Consistent with the emerging view that the brain is composed of complex, distributed networks (Power et al., 2011; Yeo et al., 2011; Petersen and Sporns, 2015), we found that individual regions within the same network exhibited relatively similar psychological profiles to each other. For example, all regions in the fronto-parietal network exhibited strong associations with executive functions, consistent with the hypothesis that the fronto-parietal network critical for flexible externally oriented behavior. In contrast, regions in different networks showed distinct psychological profiles from each other— despite occasionally high spatial proximity. For example, area ‘9’ of the default network, showed no significant association with any executive functions despite being positioned immediately dorsal to area ‘9/46’ of the fronto-parietal network. However, despite being relatively distant, areas ‘9’ and ‘47/12’ of the default network were both preferentially recruited by internally oriented processes such as ‘mentalizing’, ‘emotion’ and ‘memory’— a pattern consistent with a hypothesized role of the default network in self-generated conceptual processing (Andrews-Hanna et al., 2014).

Although networks exhibited relatively robust dissociations, within each network we observed relatively low modularity, in contrast to more localizationist

1
2
3
4
5
6
7
8
9
10
11
12
13
14
15
16
17
18
19
20
21
22
23
24
25
26
27
28
29
30
31
32
33
34
35
36
37
38
39
40
41
42
43
44
45
46
47
48
49
50
51
52
53
54
55
56
57
58
59
60

models. For example, sustained activity in DLPFC during working memory tasks has been hypothesized to reflect the active storage of working memory representations in domain-specific buffers (Baddeley, 2003). However, we find that working memory recruits activity across a wide range of regions extending from posterior LFC to the lateral frontal pole. Moreover, many of these same regions that are preferentially recruited by working memory are similarly recruited by other executive functions, such as ‘conflict’ and ‘switching’, suggesting sustained activity in these regions supports domain-general processes required to flexibly guide behavior in support of the task goals (Curtis and Lee, 2010). These findings are consistent with a recent hypothesis that working memory is supported by the distributed reactivation of representations in parietal cortex, rather than isolated and modular maintenance in DLPFC (Miller and Cohen, 2001; Postle, 2016). In the same vein, updating task representations during task set switching has been hypothesized to preferentially recruit the inferior frontal junction (Derrfuss et al., 2005; Muhle-Karbe et al., 2016). However, we find that ‘switching’ preferentially recruits activity across a wide variety of LFC subregions as far rostral as the frontal pole, suggesting task-set switching is supported by distributed regions across the fronto-parietal network.

Importantly, although we observed relatively low functional specialization for individual regions across LFC, the present findings do not negate the idea that local neuron populations may be functionally specific. On the contrary, extensive neurophysiological data suggests association cortex contains overlapping neuron

populations with distinct—and often highly specific—functional profiles (Tye and Deisseroth, 2012; Kvitsiani et al., 2013; Xiu et al., 2014). Since subregions on the scale readily identified by fMRI likely exhibit aggregated activity across distinct neuron types, the relatively low modularity of these clusters should not be surprising. Rather, given that the distribution of distinct neuron populations likely varies across association cortex, one would expect individual regions to exhibit subtly varying associations to a wide range of psychological states.

Indeed, in the present study we observed substantial functional heterogeneity within each network and dissociable psychological profiles for regions within the same network. That is, although psychological states are not modularized into individual regions, the multivariate psychological profiles we generated for each region can be used to ascribe distinct roles for each region within the broader network. For instance, although all fronto-parietal regions were associated with various core executive functions, only IFJ showed additionally robust associations with high and low level motor function. Thus, it is plausible that IFJ may play an important role in biasing motoric representations in support of high-level goals represented in a distributed fashion throughout the network. In contrast, area 9/46v in mid-DLPFC was the region most strongly recruited by core executive processes, but showed no associations with ‘lower-level’ processes such as attention and motor function, suggesting this region may be more important for the biasing of abstract representations in more domain-specific regions of posterior cortex (Badre, 2008).

1
2
3
4
5
6
7
8
9
10
11
12
13
14
15
16
17
18
19
20
21
22
23
24
25
26
27
28
29
30
31
32
33
34
35
36
37
38
39
40
41
42
43
44
45
46
47
48
49
50
51
52
53
54
55
56
57
58
59
60

Although the present results provide a comprehensive view into the functional organization of LFC, several challenges remain. As with any attempt to model the mapping between functional and brain structure, several simplifying assumptions were made in order to generate a parsimonious solution. First, the hierarchical clustering algorithm we used forces voxels to be grouped into discrete non-overlapping regions– an assumption that ignores the vast diversity overlapping neuronal populations within each region (Tye and Deisseroth, 2012; Kvitsiani et al., 2013; Xiu et al., 2014). Second, similarly to many multivariate models in this domain, we modeled the relationship between psychological topics and activity in regions using linear correlations– an assumption that ignores possible non-linear relationships.

More broadly, a difficult challenge in cognitive neuroscience is developing the appropriate psychological constructs that distinguish activity in related brain regions. Appropriately modeling the differences between nuanced psychological concepts is particularly difficult for large-scale meta-analyses, as there is no established ontology of psychological constructs, unlike in fields such as genetics (Ashburner et al., 2000). In the present study, we used a data-driven set of topics derived from the abstracts of fMRI papers to represent major psychological phenomena. Although these topics are a major improvement on more simple term-based features, due to their data-driven nature they are likely to imperfectly capture psychological dimensions that are hypothesized to be important for differentiating regions. For example, in our set of 60 topics, only a single topic

represented long-term memory function, and likely combined memory retrieval and autobiographical memory processes. Although the Neurosynth framework allows researchers to develop custom meta-analyses that can be used to test apriori predictions, the myriad of combinations in which studies can be combined is not conducive to determining the psychological dimensions that best differentiate brain activity.

The classification-based approach we employed is a step in the direction of quantifying the extent to which a given set of psychological features explains variability in brain activity. A promising future direction is to use classification based approaches and feature engineering to find the psychological dimensions that best differentiate patterns in activity between related regions, such as regions within a network. In combination with the adoption of standardized cognitive ontologies, such as the Cognitive Atlas (Poldrack et al., 2011), such large-scale approaches should help the development of novel theories of functional brain organization. Moreover, given the limited quality of the summarized coordinate based data in Neurosynth (Salimi-Khorshidi et al., 2009) the widespread sharing of richer statistical images in databases such as NeuroVault (Gorgolewski et al., 2015) will greatly improve the fidelity of future meta-analyses.

In the present study, we used relatively unbiased data-driven methods to comprehensively map psychological states to individual regions in lateral frontal cortex. These regions were organized within large-scale whole-brain networks and

1
2
3
4
5
6
7
8
9
10
11
12
13
14
15
16
17
18
19
20
21
22
23
24
25
26
27
28
29
30
31
32
33
34
35
36
37
38
39
40
41
42
43
44
45
46
47
48
49
50
51
52
53
54
55
56
57
58
59
60

shared functional properties with other regions in the same network. Moreover, we found that various specific psychological processes that have been previously hypothesized to map onto specific brain regions were widely distributed throughout lateral frontal cortex. Yet, we identified dissociable functional profiles for each subregion, suggesting that lateral frontal cortex supports a wide variety of psychological states through a mixture of network-level dynamics and moderate degree of functional specialization.

Acknowledgments: This work was supported by the National Institutes of Health. Grant number: R01MH096906.

References

- Andrews-Hanna JR (2012) The Brain's Default Network and Its Adaptive Role in Internal Mentation. *The Neuroscientist* 18:251–270.
- Andrews-Hanna JR, Smallwood J, Spreng RN (2014) The default network and self-generated thought: component processes, dynamic control, and clinical relevance Kingstone A, Miller MB, eds. *Ann NY Acad Sci* 1316:29–52.
- Aron AR, Robbins TW, Poldrack RA (2014) Inhibition and the right inferior frontal cortex: one decade on. *Trends in Cognitive Sciences* 18:177–185.
- Ashburner M et al. (2000) Gene ontology: tool for the unification of biology. The Gene Ontology Consortium. *Nat Genet* 25:25–29.
- Baddeley A (2003) Working memory: looking back and looking forward. *Nat Rev Neurosci* 4:829–839.
- Badre D (2008) Cognitive control, hierarchy, and the rostro–caudal organization of the frontal lobes. *Trends in Cognitive Sciences* 12:193–200.
- Badre D, Wagner AD (2007) Left ventrolateral prefrontal cortex and the cognitive control of memory. *Neuropsychologia* 45:2883–2901.
- Bertolero MA, Yeo BTT, D'Esposito M (2015) The modular and integrative functional architecture of the human brain. *Proc Natl Acad Sci USA* 112:E6798–E6807.

1
2
3
4
5
6
7
8
9
10
11
12
13
14
15
16
17
18
19
20
21
22
23
24
25
26
27
28
29
30
31
32
33
34
35
36
37
38
39
40
41
42
43
44
45
46
47
48
49
50
51
52
53
54
55
56
57
58
59
60

Binder JR, Desai RH, Graves WW, Conant LL (2009) Where Is the Semantic System? A Critical Review and Meta-Analysis of 120 Functional Neuroimaging Studies. *Cereb Cortex* 19:2767–2796.

Blei DM, Ng AY, Jordan MI (2003) Latent Dirichlet Allocation. *Journal of Machine Learning Research* 3:993–1022.

Bludau S, Eickhoff SB, Mohlberg H, Caspers S, Laird AR, Fox PT, Schleicher A, Zilles K, Amunts K (2014) Cytoarchitecture, probability maps and functions of the human frontal pole. *NeuroImage* 93 Pt 2:260–275.

Cavada C, Goldman-Rakic PS (1989) Posterior parietal cortex in rhesus monkey: I. Parcellation of areas based on distinctive limbic and sensory corticocortical connections. *J Comp Neurol* 287:393–421.

Chang LJ, Yarkoni T, Khaw MW, Sanfey AG (2013) Decoding the Role of the Insula in Human Cognition: Functional Parcellation and Large-Scale Reverse Inference. *Cereb Cortex* 23:739–749.

Chatham CH, Claus ED, Kim A, Curran T, Banich MT, Munakata Y (2012) Cognitive control reflects context monitoring, not motoric stopping, in response inhibition. *Gilbert S, ed. PLoS ONE* 7:e31546.

Curtis CE, Lee D (2010) Beyond working memory: the role of persistent activity in decision making. *Trends in Cognitive Sciences* 14:216–222.

- De Baene W, Albers AM, Brass M (2012) The what and how components of cognitive control. *NeuroImage* 63:203–211.
- Denny BT, Kober H, Wager TD, Ochsner KN (2012) A meta-analysis of functional neuroimaging studies of self- and other judgments reveals a spatial gradient for mentalizing in medial prefrontal cortex. *Journal of Cognitive Neuroscience* 24:1742–1752.
- Derrfuss J, Brass M, Neumann J, Cramon von DY (2005) Involvement of the inferior frontal junction in cognitive control: Meta-analyses of switching and Stroop studies. *Hum Brain Mapp* 25:22–34.
- Dosenbach NUF, Visscher KM, Palmer ED, Miezin FM, Wenger KK, Kang HC, Burgund ED, Grimes AL, Schlaggar BL, Petersen SE (2006) A core system for the implementation of task sets. *Neuron* 50:799–812.
- Duncan J (2010) The multiple-demand (MD) system of the primate brain: mental programs for intelligent behaviour. *Trends in Cognitive Sciences* 14:172–179.
- Eickhoff SB, Paus T, Caspers S, Grosbras M-H, Evans AC, Zilles K, Amunts K (2007) Assignment of functional activations to probabilistic cytoarchitectonic areas revisited. 36:511–521 Available at: <http://dx.doi.org/10.1016/j.neuroimage.2007.03.060>.
- Eickhoff SB, Thirion B, Varoquaux G, Bzdok D (2015) Connectivity-based parcellation: Critique and implications. *Hum Brain Mapp* 36:4771–4792.

1
2
3
4
5
6
7
8
9
10
11
12
13
14
15
16
17
18
19
20
21
22
23
24
25
26
27
28
29
30
31
32
33
34
35
36
37
38
39
40
41
42
43
44
45
46
47
48
49
50
51
52
53
54
55
56
57
58
59
60

Flinker A, Korzeniewska A, Shestyuk AY, Franaszczuk PJ, Dronkers NF, Knight RT, Crone NE (2015) Redefining the role of Broca's area in speech. *Proc Natl Acad Sci USA* 112:2871–2875.

Fodor JA (1983) *The modularity of mind: An essay on faculty psychology*. Bradford Bks.

Gilbert SJ, Spengler S, Simons JS, Steele JD, Lawrie SM, Frith CD, Burgess PW (2006) Functional specialization within rostral prefrontal cortex (area 10): a meta-analysis. *Journal of Cognitive Neuroscience* 18:932–948.

Gorgolewski KJ, Varoquaux G, Rivera G, Schwarz Y, Ghosh SS, Maumet C, Sochat VV, Nichols TE, Poldrack RA, Poline J-B, Yarkoni T, Margulies DS (2015) NeuroVault.org: a web-based repository for collecting and sharing unthresholded statistical maps of the human brain. *Front Neuroinform* 9:8.

Goulas A, Uylings HBM, Stiers P (2012) Unravelling the Intrinsic Functional Organization of the Human Lateral Frontal Cortex: A Parcellation Scheme Based on Resting State fMRI. *Journal of Neuroscience* 32:10238–10252.

Jeni LA, Cohn JF, La Torre De F (2013) Facing Imbalanced Data--Recommendations for the Use of Performance Metrics. In, pp 245–251. IEEE.

Kim J-H, Lee J-M, Jo HJ, Kim SH, Lee JH, Kim ST, Seo SW, Cox RW, Na DL, Kim SI, Saad ZS (2010) Defining functional SMA and pre-SMA subregions in human MFC using resting state fMRI: Functional connectivity-based parcellation

method. *NeuroImage* 49:2375–2386.

Kober H, Barrett LF, Joseph J, Bliss-Moreau E, Lindquist K, Wager TD (2008)

Functional grouping and cortical-subcortical interactions in emotion: a meta-analysis of neuroimaging studies. *NeuroImage* 42:998–1031.

Kober H, Wager TD (2010) *Meta-analysis of neuroimaging data*. Wiley

Interdisciplinary Reviews: Cognitive Science 1:293–300.

Kvitsiani D, Ranade S, Hangya B, Taniguchi H, Huang JZ, Kepecs A (2013) Distinct

behavioural and network correlates of two interneuron types in prefrontal cortex. *Nature* 498:363–366.

De La Vega A, Chang LJ, Banich MT, Wager TD, Yarkoni T (2016) Large-Scale

Meta-Analysis of Human Medial Frontal Cortex Reveals Tripartite Functional Organization. *J Neurosci* 36:6553–6562.

Mackey WE, Devinsky O, Doyle WK, Meager MR, Curtis CE (2016) Human

Dorsolateral Prefrontal Cortex Is Not Necessary for Spatial Working Memory. *Journal of Neuroscience* 36:2847–2856.

Miller EK, Cohen JD (2001) An integrative theory of prefrontal cortex function.

Annu Rev Neurosci 24:167–202.

Miyake A, Friedman NP, Emerson MJ, Witzki AH, Howerter A, Wager TD (2000)

The unity and diversity of executive functions and their contributions to

1
2
3
4
5
6
7
8
9
10
11
12
13
14
15
16
17
18
19
20
21
22
23
24
25
26
27
28
29
30
31
32
33
34
35
36
37
38
39
40
41
42
43
44
45
46
47
48
49
50
51
52
53
54
55
56
57
58
59
60

complex “Frontal Lobe” tasks: a latent variable analysis. *Cogn Psychol* 41:49–100.

Muhle-Karbe PS, Derrfuss J, Lynn MT, Neubert FX, Fox PT, Brass M, Eickhoff SB (2016) Co-Activation-Based Parcellation of the Lateral Prefrontal Cortex Delineates the Inferior Frontal Junction Area. *Cereb Cortex* 26:2225–2241.

Müllner D (2013) fastcluster: Fast hierarchical, agglomerative clustering routines for R and Python. *Journal of Statistical Software*.

Nee DE, Brown JW (2012) Rostral–caudal gradients of abstraction revealed by multi-variate pattern analysis of working memory. *NeuroImage* 63:1285–1294.

Nee DE, Brown JW, Askren MK, Berman MG, Demiralp E, Krawitz A, Jonides J (2013) A Meta-analysis of Executive Components of Working Memory. *Cereb Cortex* 23:264–282.

Nee DE, Wager TD, Jonides J (2007) Interference resolution: insights from a meta-analysis of neuroimaging tasks. *Cogn Affect Behav Neurosci* 7:1–17.

Nelson SM, Dosenbach NUF, Cohen AL, Wheeler ME, Schlaggar BL, Petersen SE (2010) Role of the anterior insula in task-level control and focal attention. *Brain Struct Funct* 214:669–680.

Neubert F-X, Mars RB, Sallet J, Rushworth MFS (2015) Connectivity reveals relationship of brain areas for reward-guided learning and decision making in

human and monkey frontal cortex. *Proceedings of the National Academy of Sciences* 112:E2695–E2704.

Orr JM, Smolker HR, Banich MT (2015) Organization of the Human Frontal Pole Revealed by Large-Scale DTI-Based Connectivity: Implications for Control of Behavior. *PLoS ONE* 10:e0124797.

Pauli WM, O'Reilly RC, Yarkoni T, Wager TD (2016) Regional specialization within the human striatum for diverse psychological functions. *Proc Natl Acad Sci USA* 113:1907–1912.

Paus T (1996) Location and function of the human frontal eye-field: a selective review. *Neuropsychologia* 34:475–483.

Pedregosa F, Varoquaux G, Gramfort A, Michel V, Thirion B, Grisel O, Blondel M, Prettenhofer P, Weiss R, Dubourg V, Vanderplas J, Passos A, Cournapeau D, Brucher M, Perrot M, Duchesnay É (2011) Scikit-learn: Machine Learning in Python. *Journal of Machine Learning Research* 12:2825–2830.

Petersen SE, Sporns O (2015) Brain Networks and Cognitive Architectures. *Neuron* 88:207–219.

Petrides M (2005) Lateral prefrontal cortex: architectonic and functional organization. *Philosophical Transactions of the Royal Society B: Biological Sciences* 360:781–795.

1
2
3
4
5
6
7
8
9
10
11
12
13
14
15
16
17
18
19
20
21
22
23
24
25
26
27
28
29
30
31
32
33
34
35
36
37
38
39
40
41
42
43
44
45
46
47
48
49
50
51
52
53
54
55
56
57
58
59
60

Petrides M, Pandya DN (1984) Projections to the frontal cortex from the posterior parietal region in the rhesus monkey. *J Comp Neurol* 228:105–116.

Poldrack RA (2006) Can cognitive processes be inferred from neuroimaging data? *Trends in Cognitive Sciences* 10:59–63.

Poldrack RA, Kittur A, Kalar D, Miller E, Seppa C, Gil Y, Parker DS, Sabb FW, Bilder RM (2011) The cognitive atlas: toward a knowledge foundation for cognitive neuroscience. *Front Neuroinform* 5:17.

Poldrack RA, Mumford JA, Schonberg T, Kalar D, Barman B, Yarkoni T (2012) Discovering Relations Between Mind, Brain, and Mental Disorders Using Topic Mapping Sporns O, ed. *PLoS Comput Biol* 8:e1002707–e1002714.

Postle BR (2016) Working memory functions of the prefrontal cortex. In, pp 1–14.

Power JD, Cohen AL, Nelson SM, Wig GS, Barnes KA, Church JA, Vogel AC, Laumann TO, Miezin FM, Schlaggar BL, Petersen SE (2011) Functional network organization of the human brain. *Neuron* 72:665–678.

Salimi-Khorshidi G, Smith SM, Keltner JR, Wager TD, Nichols TE (2009) Meta-analysis of neuroimaging data: a comparison of image-based and coordinate-based pooling of studies. *NeuroImage* 45:810–823.

Sallet J, Mars RB, Noonan MP, Neubert F-X, Jbabdi S, O'Reilly JX, Filippini N, Thomas AG, Rushworth MF (2013) The organization of dorsal frontal cortex in

humans and macaques. *J Neurosci* 33:12255–12274.

Snyder HR, Banich MT, Munakata Y (2011) Choosing our words: retrieval and selection processes recruit shared neural substrates in left ventrolateral prefrontal cortex. *Journal of Cognitive Neuroscience* 23:3470–3482.

Thirion B, Varoquaux G, Dohmatob E, Poline J-B (2014) Which fMRI clustering gives good brain parcellations? *Front Neurosci* 8:169.

Toro R, Fox PT, Paus T (2008) Functional coactivation map of the human brain. *Cereb Cortex* 18:2553–2559.

Tye KM, Deisseroth K (2012) Optogenetic investigation of neural circuits underlying brain disease in animal models. *Nat Rev Neurosci* 13:251–266.

Wager TD, Davidson ML, Hughes BL, Lindquist MA, Ochsner KN (2008) Prefrontal-subcortical pathways mediating successful emotion regulation. *Neuron* 59:1037–1050.

Wager TD, Jonides J, Reading S (2004) Neuroimaging studies of shifting attention: a meta-analysis. *NeuroImage* 22:1679–1693.

Wager TD, Kang J, Johnson TD, Nichols TE, Satpute AB, Barrett LF (2015) A Bayesian model of category-specific emotional brain responses. *PLoS Comput Biol* 11:e1004066.

Wager TD, Smith EE (2003) Neuroimaging studies of working memory: a meta-

1
2
3
4
5
6
7
8
9
10
11
12
13
14
15
16
17
18
19
20
21
22
23
24
25
26
27
28
29
30
31
32
33
34
35
36
37
38
39
40
41
42
43
44
45
46
47
48
49
50
51
52
53
54
55
56
57
58
59
60

analysis. *Cogn Affect Behav Neurosci* 3:255–274.

Woo C-W, Koban L, Kross E, Lindquist MA, Banich MT, Ruzic L, Andrews-Hanna JR, Wager TD (2014) Separate neural representations for physical pain and social rejection. *Nature Communications* 5:5380.

Xiu J, Zhang Q, Zhou T, Zhou T-T, Zhou T, Chen Y, Hu H (2014) Visualizing an emotional valence map in the limbic forebrain by TAI-FISH. *Nat Neurosci* 17:1552–1559.

Yarkoni T, Poldrack RA, Nichols TE, Van Essen DC, Wager TD (2011) Large-scale automated synthesis of human functional neuroimaging data. *Nat Methods* 8:665–670.

Yeo BT, Krienen FM, Sepulcre J, Sabuncu MR, Lashkari D, Hollinshead M, Roffman JL, Smoller JW, Zollei L, Polimeni JR, Fischl B, Liu H, Buckner RL (2011) The organization of the human cerebral cortex estimated by intrinsic functional connectivity. *Journal of Neurophysiology* 106:1125–1165.

Topic name	Top words
action	action actions motor goal mirror planning imitation execution
attention	attention attentional visual spatial search location orienting target
conflict	conflict interference incongruent stroop congruent selection competition color
emotion	emotional emotion regulation affective pictures emotions arousal affect
gaze	eye gaze eyes movements saccades target saccade visual
inhibition	inhibition inhibitory stop motor sustained nogo transient suppression
memory	memory retrieval encoding recognition episodic items recall words
mentalizing	social empathy moral person judgments mentalizing mental mind
motor	motor movement movements sensorimotor finger somatosensory sensory force
novelty	target targets novelty oddball distractor distractors deception mismatch
pain	pain stimulation somatosensory painful intensity sensory chronic noxious
reward	reward sleep anticipation monetary rewards motivation incentive loss
semantics	semantic words word lexical verbs abstract meaning verb
speech	speech auditory sounds sound perception voice acoustic listening
switching	switching rule executive switch rules flexibility shifting aggression
WM	memory working wm load verbal maintenance delay encoding

Table 1. Topics most strongly associated with lateral frontal regions. Eight strongest loading words for each topic are listed, in descending order of association strength.

Figure 1. Methods overview. a) We calculated co-activation across studies between every cortical voxel and the rest of the brain, including subcortex. We then applied Ward hierarchical clustering to obtain whole-brain clustering results. We chose two spatial scales to focus on using the silhouette method (Kober et al., 2008; Pauli et al., 2016) and selected clusters in LFC from the whole-brain clustering solutions. b) We contrasted the whole-brain co-activation of each cluster with LFC at large, identifying voxels across the brain that showed differential co-activation. c) We generated functional preference profiles for each cluster by determining which latent psychological topics (Blei et al., 2003) best predicted the cluster's activation

1
2
3
4
5
6
7
8
9
10
11
12
13
14
15
16
17
18
19
20
21
22
23
24
25
26
27
28
29
30
31
32
33
34
35
36
37
38
39
40
41
42
43
44
45
46
47
48
49
50
51
52
53
54
55
56
57
58
59
60

across studies in the database.

Figure 2. Whole-cortex co-activation based hierarchical clustering reveals 3 networks in lateral cluster that fractionate into constituent subregions. a) The silhouette score, a measure of intra-cluster cohesion, was used to select two spatial scales: 5 and 70 whole-brain clusters. b) Whole brain hierarchical clustering dendrogram. Color-coded branches correspond to three of five whole-brain networks in LFC and color-coded nodes correspond to 14 LFC regions from 70 whole-brain clusters. c) Clusters at $k = 5$ revealed three clusters in LFC resembling large-scale brain networks: “fronto-parietal” (red), “default” (purple) and “somatosensory-motor” (green) d) Clusters at $k = 70$ revealed 14 clusters with a 75% of their voxels in LFC.

Figure 3. Anatomical location and meta-analytic contrast of lateral frontal clusters of the fronto-parietal network. Left: a) Two clusters located in caudal frontal cortex. b) Four clusters located in mid-lateral pre-frontal cortex. c) Three clusters located in rostral lateral pre-frontal cortex. Clusters were assigned labels corresponding to cytoarchitectonic areas (Petrides, 2005) whenever possible. In cases where the region spanned multiple cytoarchitectonic areas, broader anatomical (e.g. inferior frontal junction [IFJ]) labels were assigned. Right: Meta-analytic co-activation contrast of fronto-parietal LFC. Colored voxels indicate significantly greater co-activation with the seed region of the same color than other lateral frontal regions in the fronto-parietal network. Images are presented using neurological convention and are corrected using false discovery rate (FDR; $q = 0.01$).

Figure 4. Meta-analytic functional preference profiles for lateral frontal regions in the fronto-parietal network.

Each cluster was profiled to determine which psychological topics best predicted its activation. Each of the three functional groups we identified showed distinct functional profiles, although appreciable variation was observed for each individual cluster. Strength of association is measured in log odds-ratio (LOR), and permutation-based significance corrected using false discovery rate (FDR) of $q = 0.01$ is indicated next to each psychological concept by color-coded dots corresponding to each region. Negative associations are indicated by the grey circle.

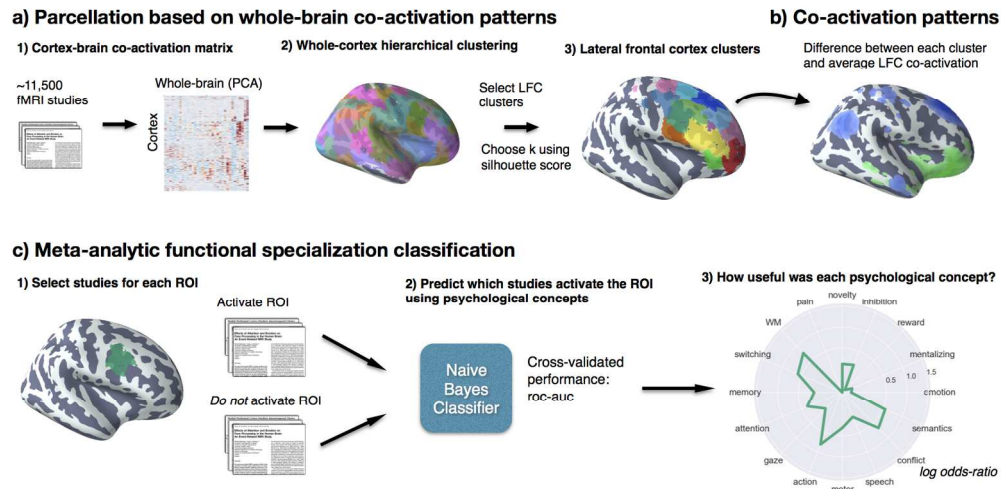
Figure 5. Lateral frontal regions of the default network a) Individual clusters projected onto an inflated surface. b) Differences in co-activation between the three regions. Colored voxels activated more frequently in studies in the seed cluster of the same color was also active. c) Functional preference profiles for each cluster, revealing distinct psychological signatures for each subregion. Strength of association is measured in log odds-ratio (LOR), and permutation-based significance is indicated next to each topic by color-coded dots corresponding to each region. Negative associations are indicated by the grey circle.

Figure 6. Meta-analysis of somatosensory clusters. a) Clusters projected onto an inflated surface b) Differences in co-activation between each cluster and the rest of LFC. Colored voxels activated more frequently in studies in which the seed cluster of the same color was also active. c) Functional preference profiles reveal distinct

1
2
3
4
5
6
7
8
9
10
11
12
13
14
15
16
17
18
19
20
21
22
23
24
25
26
27
28
29
30
31
32
33
34
35
36
37
38
39
40
41
42
43
44
45
46
47
48
49
50
51
52
53
54
55
56
57
58
59
60

psychological signatures. Strength of association is measured in log odds-ratio (LOR), and permutation-based significance ($q < 0.05$) is indicated next to each topic by color-coded dots corresponding to each cluster. Negative associations are indicated by the grey circle

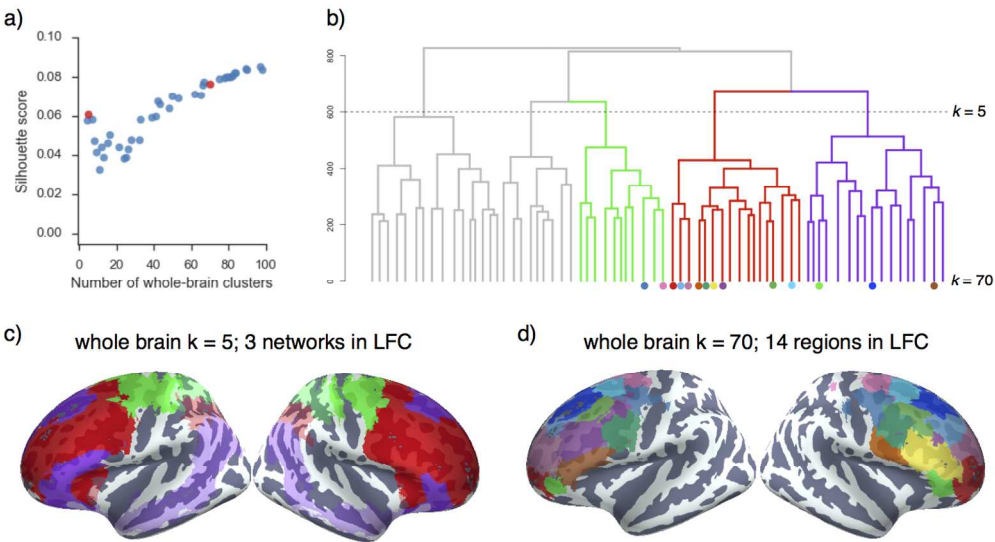
Figure 7. Co-activation and functional distance between LFC clusters. Pearson's correlation distance between the 14 LFC clusters on the basis of meta-analytic (a) co-activation and (b) functional preference profiles. Although clusters within each network showed generally shorter distances to clusters in the same network than between networks, relatively high functional heterogeneity within each network was observed. The high similarities between these two distance matrices ($r = 0.86$, $p < 0.001$), suggests that the differences between regions observed in meta-analytic co-activation are generally accompanied by differences in functional preference profiles. Correlation distances range from 0 to 2, with 2 indicating perfect anti-correlation.



Methods overview. a) We calculated co-activation across studies between every cortical voxel and the rest of the brain, including subcortex. We then applied Ward hierarchical clustering to obtain whole-brain clustering results. We chose two spatial scales to focus on using the silhouette method (Kober et al., 2008; Pauli et al., 2016) and selected clusters in LFC from the whole-brain clustering solutions. b) We contrasted the whole-brain co-activation of each cluster with LFC at large, identifying voxels across the brain that showed differential co-activation. c) We generated functional preference profiles for each cluster by determining which latent psychological topics (Blei et al., 2003) best predicted the cluster's activation across studies in the database.

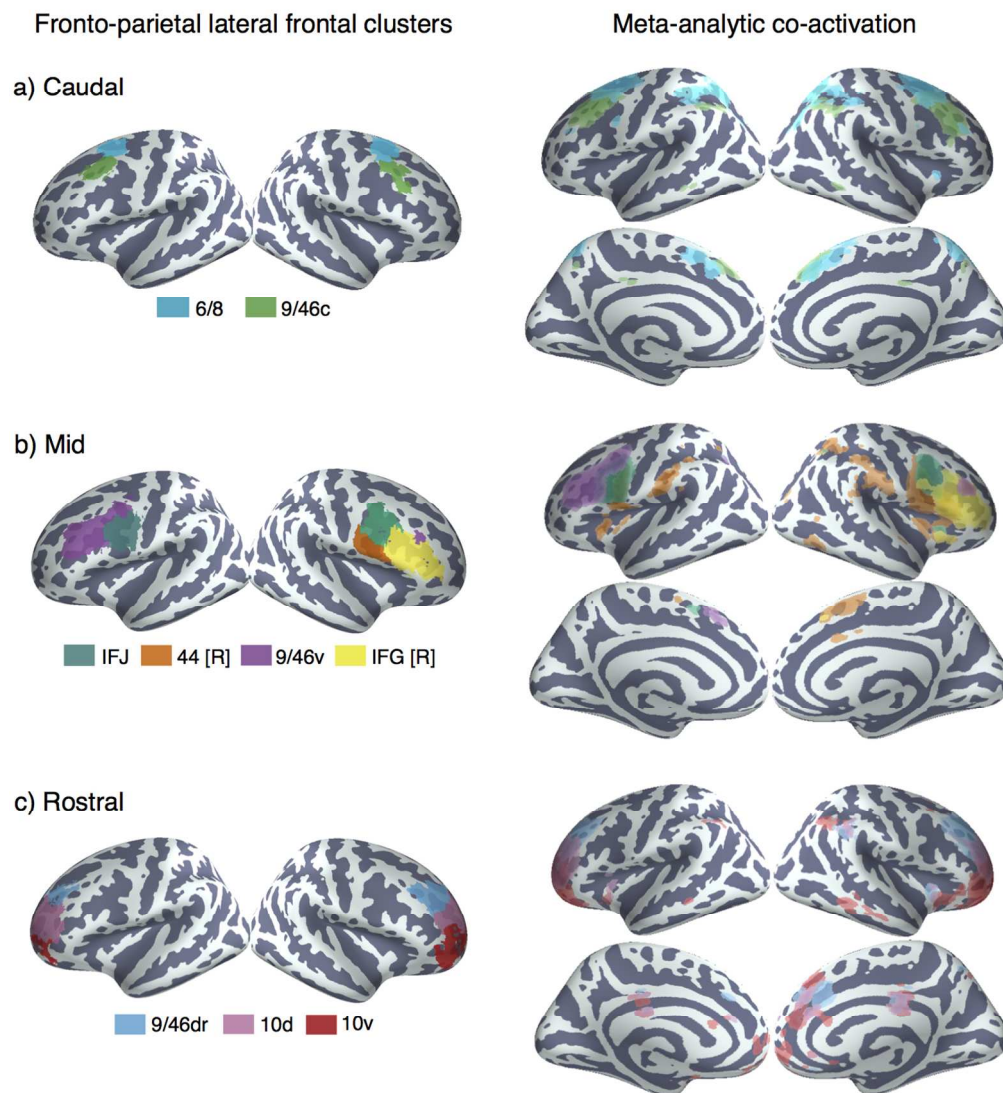
Figure 1

330x165mm (150 x 150 DPI)



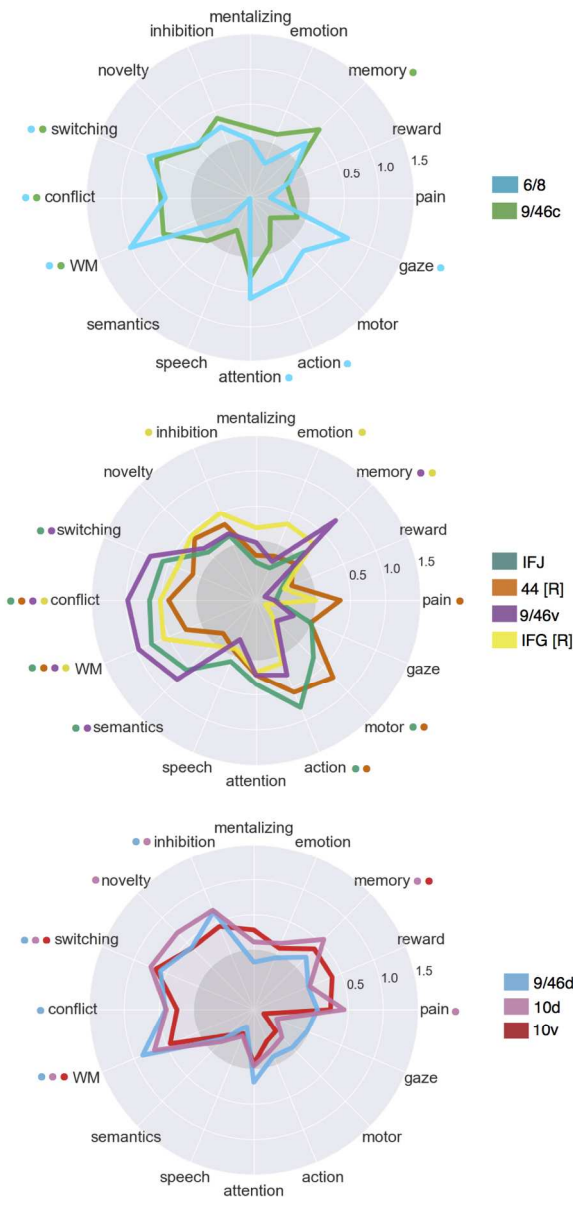
Whole-cortex co-activation based hierarchical clustering reveals 3 networks in lateral cluster that fractionate into constituent subregions. a) The silhouette score, a measure of intra-cluster cohesion, was used to select two spatial scales: 5 and 70 whole-brain clusters. b) Whole brain hierarchical clustering dendrogram. Color-coded branches correspond to three of five whole-brain networks in LFC and color-coded nodes correspond to 14 LFC regions from 70 whole-brain clusters. c) Clusters at $k = 5$ revealed three clusters in LFC resembling large-scale brain networks: “fronto-parietal” (red), “default” (purple) and “somatosensory-motor” (green) d) Clusters at $k = 70$ revealed 14 clusters with a 75% of their voxels in LFC.

Figure 2
271x152mm (150 x 150 DPI)



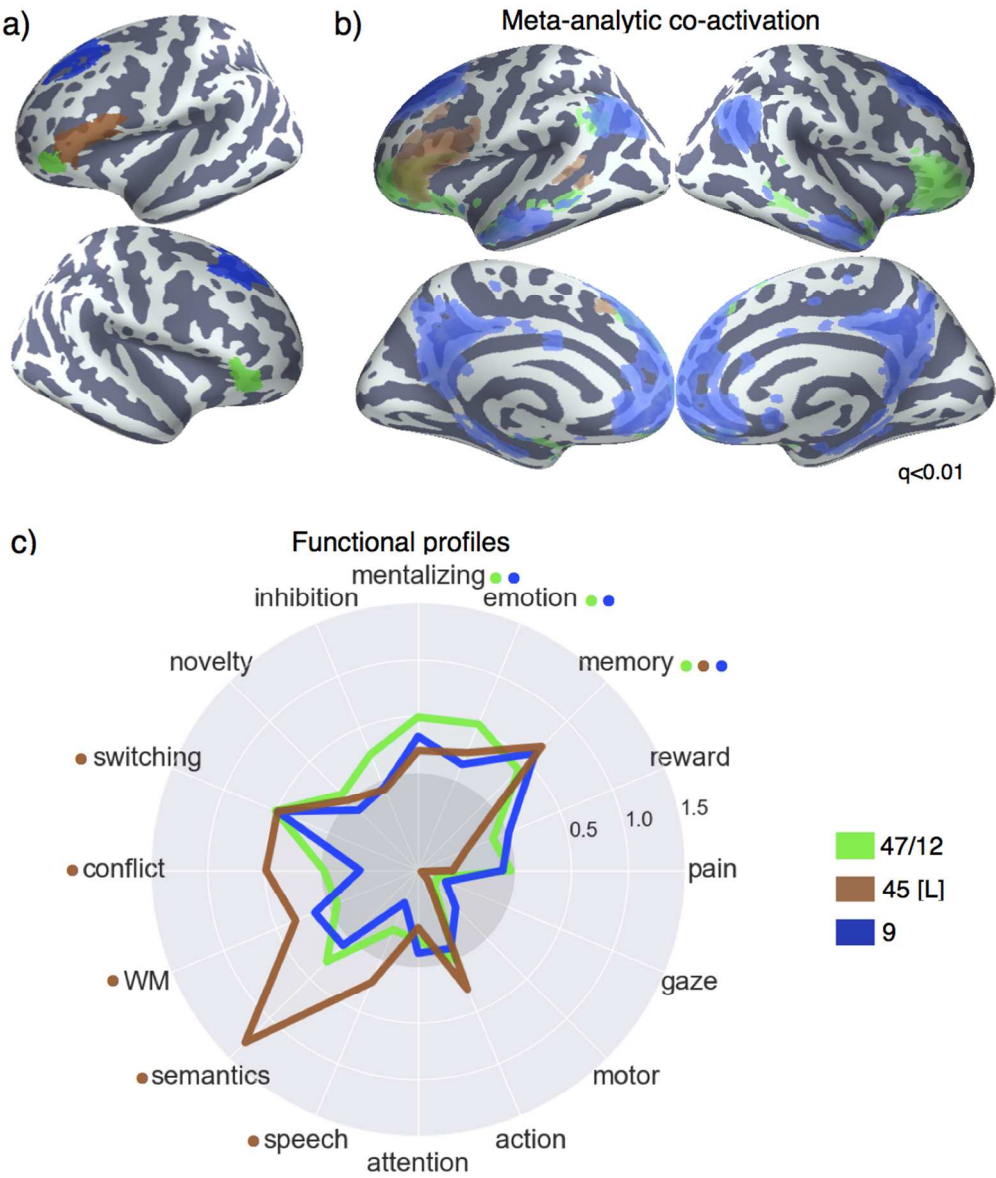
Anatomical location and meta-analytic contrast of lateral frontal clusters of the fronto-parietal network. Left: a) Two clusters located in caudal frontal cortex. b) Four clusters located in mid-lateral pre-frontal cortex. c) Three clusters located in rostral lateral pre-frontal cortex. Clusters were assigned labels corresponding to cytoarchitectonic areas (Petrides, 2005) whenever possible. In cases where the region spanned multiple cytoarchitectonic areas, broader anatomical (e.g. inferior frontal junction [IFJ]) labels were assigned. Right: Meta-analytic co-activation contrast of fronto-parietal LFC. Colored voxels indicate significantly greater co-activation with the seed region of the same color than other lateral frontal regions in the fronto-parietal network. Images are presented using neurological convention and are corrected using false discovery rate (FDR; $q = 0.01$).

Figure 3
247x279mm (150 x 150 DPI)



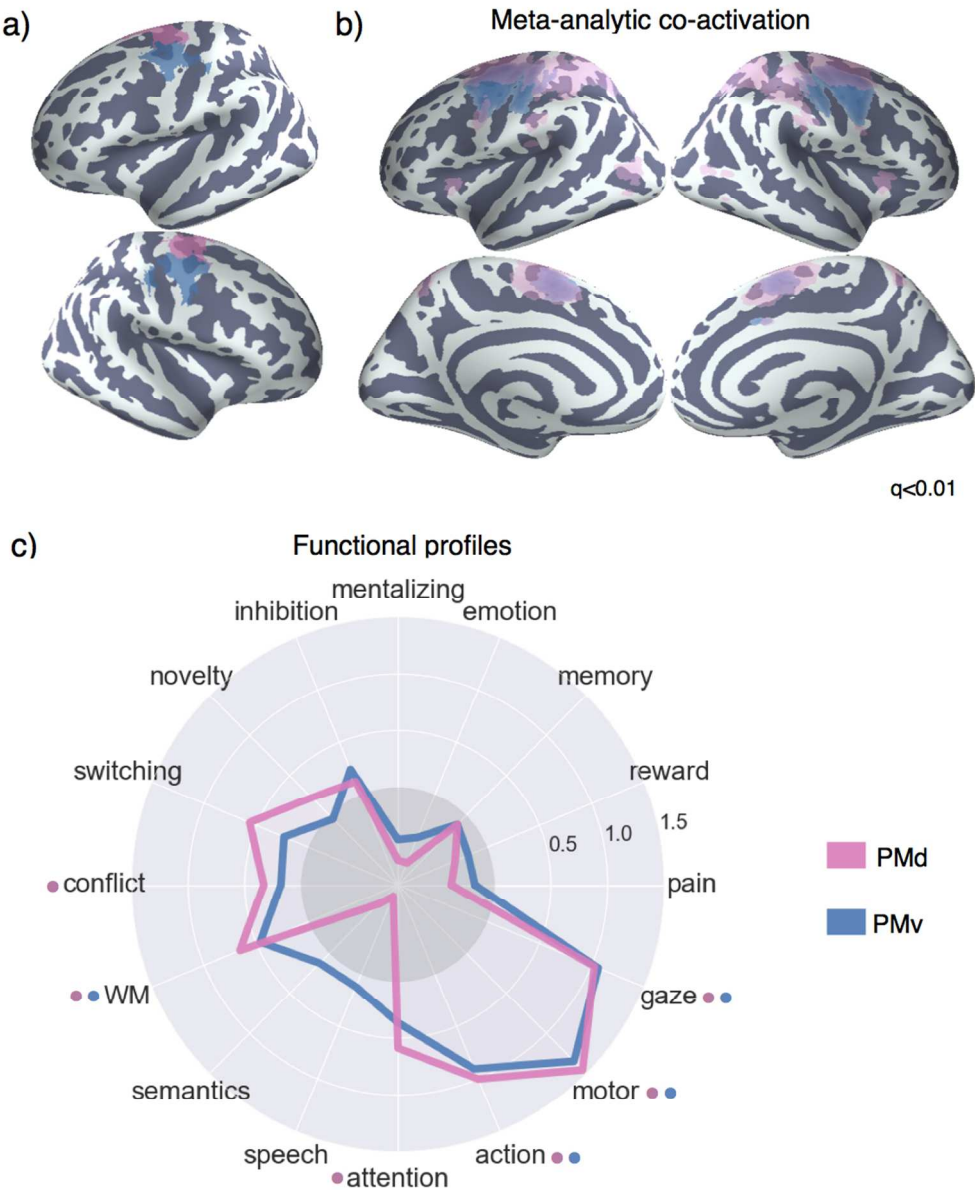
. Meta-analytic functional preference profiles for lateral frontal regions in the fronto-parietal network. Each cluster was profiled to determine which psychological topics best predicted its activation. Each of the three functional groups we identified showed distinct functional profiles, although appreciable variation was observed for each individual cluster. Strength of association is measured in log odds-ratio (LOR), and permutation-based significance corrected using false discovery rate (FDR) of $q = 0.01$ is indicated next to each psychological concept by color-coded dots corresponding to each region. Negative associations are indicated by the grey circle.

Figure 4
177x368mm (150 x 150 DPI)



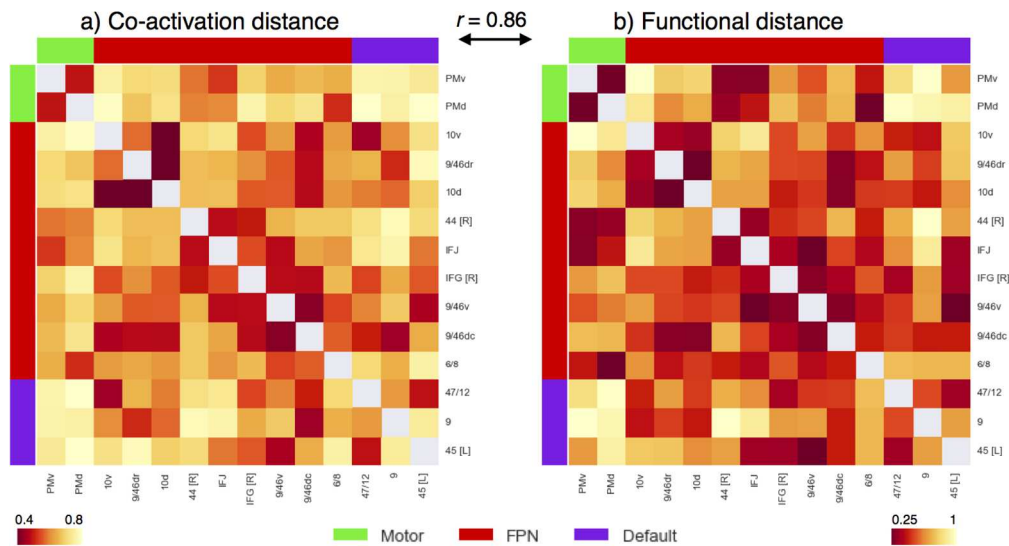
Lateral frontal regions of the default network a) Individual clusters projected onto an inflated surface. b) Differences in co-activation between the three regions. Colored voxels activated more frequently in studies in the seed cluster of the same color was also active. c) Functional preference profiles for each cluster, revealing distinct psychological signatures for each subregion. Strength of association is measured in log odds-ratio (LOR), and permutation-based significance is indicated next to each topic by color-coded dots corresponding to each region. Negative associations are indicated by the grey circle.

Figure 5
196x234mm (150 x 150 DPI)



Meta-analysis of somatosensory clusters. a) Clusters projected onto an inflated surface b) Differences in co-activation between each cluster and the rest of LFC. Colored voxels activated more frequently in studies in which the seed cluster of the same color was also active. c) Functional preference profiles reveal distinct psychological signatures. Strength of association is measured in log odds-ratio (LOR), and permutation-based significance ($q<0.05$) is indicated next to each topic by color-coded dots corresponding to each cluster. Negative associations are indicated by the grey circle.

Figure 6
196x234mm (150 x 150 DPI)

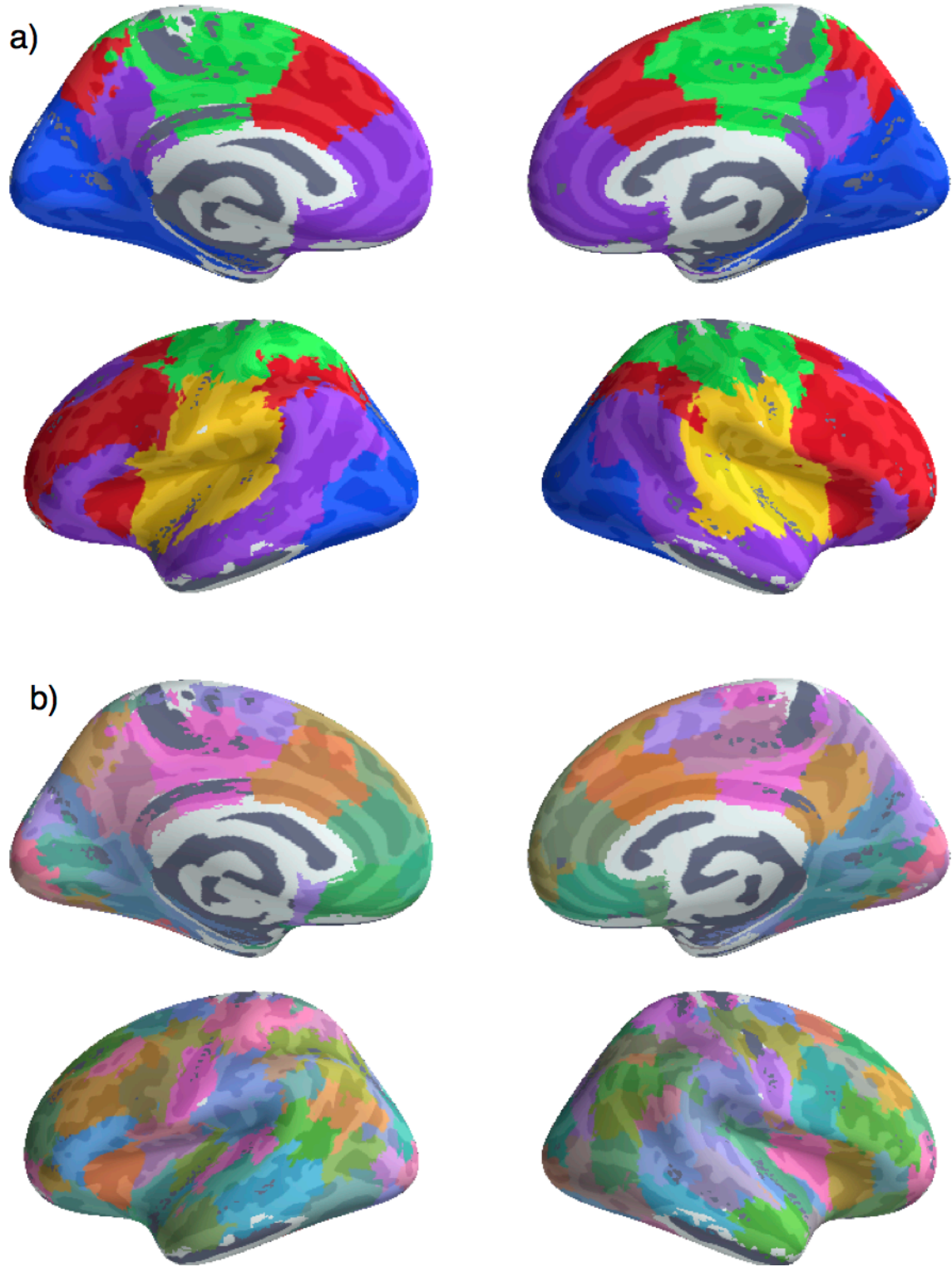


Co-activation and functional distance between LFC clusters. Pearson's correlation distance between the 14 LFC clusters on the basis of meta-analytic (a) co-activation and (b) functional preference profiles. Although clusters within each network showed generally shorter distances to clusters in the same network than between networks, relatively high functional heterogeneity within each network was observed. The high similarities between these two distance matrices ($r = 0.86$, $p < 0.001$), suggests that the differences between regions observed in meta-analytic co-activation are generally accompanied by differences in functional preference profiles. Correlation distances range from 0 to 2, with 2 indicating perfect anti-correlation.

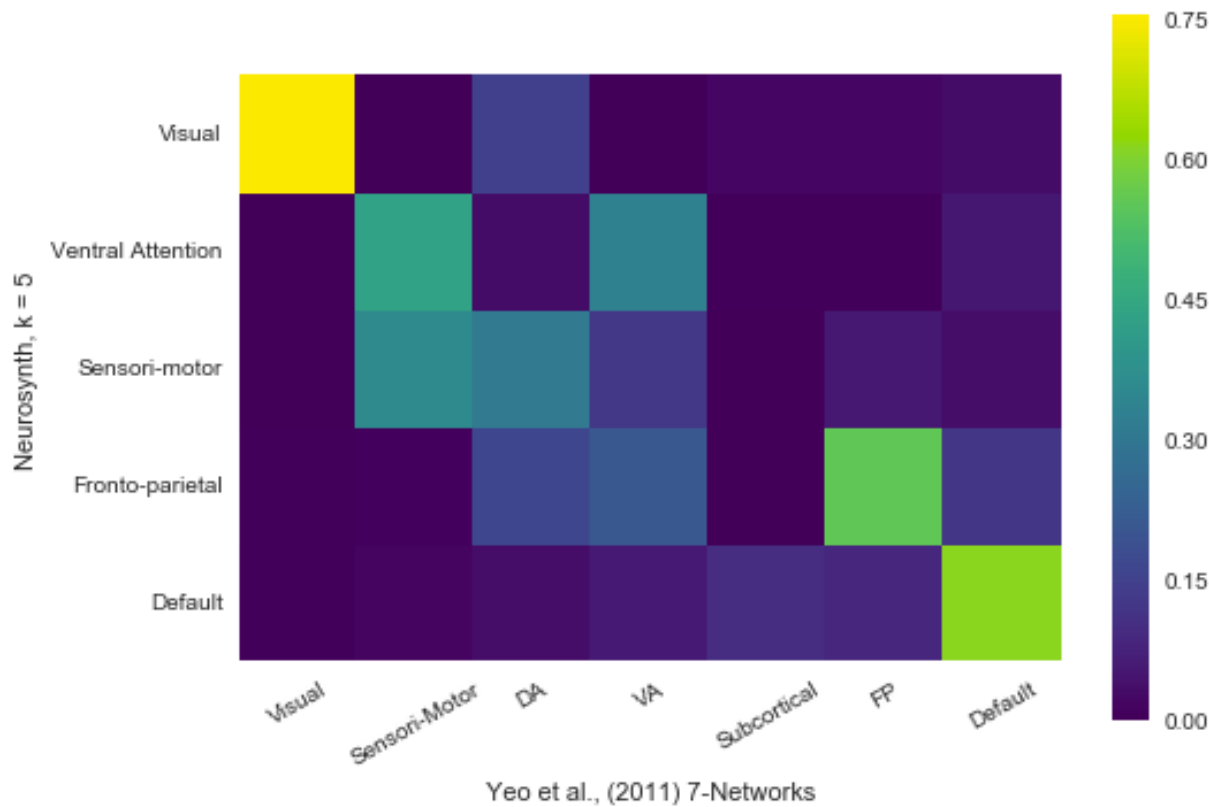
Figure 7
270x147mm (150 x 150 DPI)

Supplementary Information

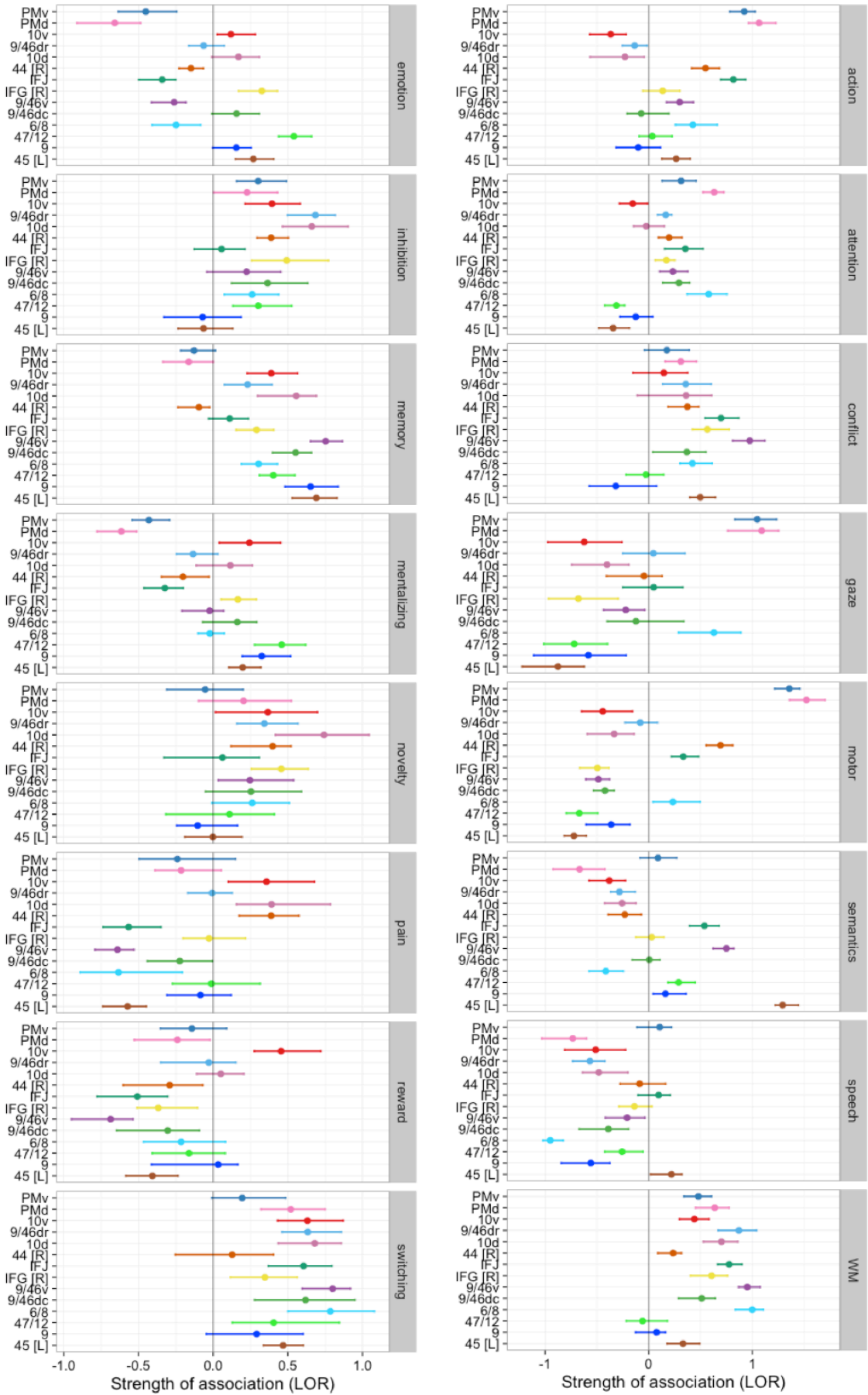
Large-scale meta-analysis suggests low regional modularity in lateral frontal cortex.



Supplemental Figure 1. Whole brain hierarchical clustering results at $k=5$ and $k=70$. In addition to the three clusters in LFC, we identified two clusters primarily outside of LFC, which we refer to as the “ventral attention” network (yellow), and the “visual” network (blue).



Supplemental Figure 2. Cross-reference of the Dice coefficient overlap between our clusters at $k = 5$ and Yeo et al., (2011)'s 7-Network solution (liberal). Greater dice coefficients indicate greater spatial overlap. Overall, there was substantial overlap between the two sets of clusters. Due to the lower dimensionality of our parcellation, some clusters (e.g. sensori-motor) showed moderated to more than one of Yeo's networks.



Supplemental Figure 3. Strength of association between the 16 topics analyzed throughout the manuscript and individual LFC sub-regions, measured as log odds ratio (LOR). 95% confidence intervals for LORs were generated by bootstrapping the full set of studies 1000 times. Colors for each region correspond to those used throughout the main text.

For Peer Review